



**US Army Corps  
of Engineers®**  
Engineer Research and  
Development Center

*Strategic Environmental Research and Development Program*

## **Photochemical Degradation of Composition B and Its Components**

Judith C. Pennington, Kevin A. Thorn, Larry G. Cox,  
Denise K. MacMillan, Sally Yost, and Randy D. Laubscher

September 2007

# **Photochemical Degradation of Composition B and Its Components**

Judith C. Pennington, Denise K. MacMillan

*Environmental Laboratory  
U.S. Army Engineer Research and Development Center  
3909 Halls Ferry Road  
Vicksburg, MS 39180-6199*

Kevin A. Thorn, Larry G. Cox

*National Water Quality Laboratory  
U.S. Geological Survey  
PO Box 25046  
Denver Federal Center, Bldg 95, MS 408  
Denver, CO 80225*

Sally Yost, Randy D. Laubscher

*Spec Pro  
4815 Bradford Drive, Suite 201  
Huntsville, AL 35805*

Final report

Approved for public release; distribution is unlimited.

**Abstract:** Products of photodecomposition of 2,4,6-trinitrotoluene (TNT) have been observed as a coating on TNT particles and as a fine powdered residue surrounding TNT particles on ranges receiving limited rainfall. The significance of photolysis of explosive formulations on training ranges is unknown. Therefore, photolysis of a common explosive formulation, Composition B, and its components in a soil matrix were evaluated. Objectives included determination of photolysis rates, effects of light intensity and duration, effects of moisture on photolysis, and identification of photolysis products. Irradiations were performed in laboratory microcosms under controlled conditions. Solutions, solids, and both solutions and solid explosives spiked into soils were irradiated. Two approaches were used to characterize products: liquid chromatography/mass spectrometry and a combination of solid and liquid state  $^{13}\text{C}$  and  $^{15}\text{N}$  nuclear magnetic resonance (NMR), and liquid state  $^1\text{H}$  NMR. Irradiation of TNT in the aqueous phase generated dramatically more photolysis products than were previously reported. The most prominent nitrogen-containing functional groups, exclusive of unreacted nitro groups, were azoxy, amide, nitrile, and azo nitrogens. Results suggest that Composition B photolysis, particularly the TNT component, generates a dynamic mixture of products and ions beginning on the solid surfaces before dissolution, and increasing once in solution phase.

**DISCLAIMER:** The contents of this report are not to be used for advertising, publication, or promotional purposes. Citation of trade names does not constitute an official endorsement or approval of the use of such commercial products. All product names and trademarks cited are the property of their respective owners. The findings of this report are not to be construed as an official Department of the Army position unless so designated by other authorized documents.

**DESTROY THIS REPORT WHEN NO LONGER NEEDED. DO NOT RETURN IT TO THE ORIGINATOR.**

# Contents

<b>Figures and Tables</b> .....	<b>iv</b>
<b>Preface</b> .....	<b>vi</b>
<b>Acronyms</b> .....	<b>vii</b>
<b>1 Introduction</b> .....	<b>1</b>
Background .....	1
Objectives .....	7
Approach.....	7
<b>2 Materials and Methods</b> .....	<b>9</b>
Irradiation .....	9
<i>Aqueous-phase irradiations: T<sup>15</sup>NT and unlabeled TNT</i> .....	10
<i>Aqueous-phase irradiations: Solvent fractionation of T<sup>15</sup>NT photolysate</i> .....	10
<i>Irradiation of solution explosives in soils</i> .....	10
<i>Irradiation of solids</i> .....	12
<i>Irradiation of solid explosives in soils, wet and dry</i> .....	12
Liquid chromatograph/mass spectrometry analysis of soils and solids.....	13
Nuclear magnetic resonance spectrometry.....	14
<b>3 Results</b> .....	<b>16</b>
Aqueous-phase irradiation.....	16
<i>NMR spectra of photolysates</i> .....	16
<i>Spectra of solvent fractionated T<sup>15</sup>NT solvent</i> .....	24
<i>Photodegradation of T<sup>15</sup>NT in presence of natural organic matter</i> .....	31
Conclusions based on NMR analyses of aqueous-phase irradiations .....	31
Solid-phase irradiations .....	33
<i>Liquid chromatograph/mass spectrometry</i> .....	33
Nuclear magnetic resonance spectrometry.....	44
<i>TNT, RDX, and Composition B solids treatments</i> .....	44
<i>TNT solution treatment</i> .....	45
<b>4 Conclusions</b> .....	<b>49</b>
<b>References</b> .....	<b>51</b>
<b>Report Documentation Page</b>	

## Figures and Tables

### Figures

Figure 1. Solid state CP/MAS $^{13}\text{C}$ NMR spectrum of 1-hour $\text{T}^{15}\text{NT}$ photolysate. ....	17
Figure 2. Continuous decoupled liquid state $^{13}\text{C}$ NMR spectra of 1-hour $\text{T}^{15}\text{NT}$ photolysate. ....	18
Figure 3. Solid state CP/MAS $^{15}\text{N}$ NMR spectrum of 1-hour $\text{T}^{15}\text{NT}$ photolysate. ....	19
Figure 4. Quantitative inverse gated decoupled liquid state $^{15}\text{N}$ NMR spectra of $\text{T}^{15}\text{NT}$ standard, 1-hour photolysate, and 16-hour photolysate. ....	20
Figure 5. Vertical scale expansions of quantitative inverse gated decoupled liquid state $^{15}\text{N}$ NMR spectra of 1- and 16-hour $\text{T}^{15}\text{NT}$ photolysates. ....	23
Figure 6. Solid state CP/MAS $^{13}\text{C}$ NMR spectra of 1-, 4-, 8-, and 16-hour TNT photolysates and TNT standard. ....	25
Figure 7. Continuous decoupled liquid state $^{13}\text{C}$ NMR spectra of 1- and 16-hour $\text{T}^{15}\text{NT}$ photolysates. ....	26
Figure 8. Liquid state $^1\text{H}$ NMR spectra of solvent fractionated 1-hour $\text{T}^{15}\text{NT}$ photolysate. ....	27
Figure 9. Liquid state $^1\text{H}$ NMR spectrum of toluene fraction from $\text{T}^{15}\text{NT}$ photolysate. ....	28
Figure 10. Liquid state $^1\text{H}$ NMR spectrum of ether I fraction from $\text{T}^{15}\text{NT}$ photolysate. ....	28
Figure 11. Liquid state $^1\text{H}$ NMR spectrum of acetonitrile fraction from $\text{T}^{15}\text{NT}$ photolysate. ....	29
Figure 12. Liquid state acoustic $^{15}\text{N}$ NMR spectra of solvent fractionated 1-hour $\text{T}^{15}\text{NT}$ photolysate. ....	30
Figure 13. Liquid state inverse gated decoupled $^{15}\text{N}$ NMR spectra of 1-hour $\text{T}^{15}\text{NT}$ photolysates in presence and absence of SRNOM, and 16-hour $\text{T}^{15}\text{NT}$ photolysate. ....	32
Figure 14. Ion profiles for selected anion of $m/z$ 226, anions in range of $m/z$ 300-400, and anions in range of $m/z$ 400-600 are presented for four representative TNT treatments. ....	34
Figure 15. Abundance of ADNT isomers, the ion of $m/z$ 256, relative to TNT abundance, in <i>TNT Solution</i> and <i>Composition B (Comp B) Solution</i> controls and samples exposed to light for 15 days. ....	36
Figure 16. Selected spectra of <i>TNT Solution</i> treatments. ....	37
Figure 17. Abundance of unknown ion of $m/z$ 264 relative to RDX in photolysis of <i>RDX Solids</i> and <i>Wet RDX</i> . ....	39
Figure 18. Abundance of aminodinitrobenzoic acid as the anion $m/z$ 226, relative to TNT in <i>TNT Solids</i> and <i>Composition B (Comp B) Solids</i> treatments exposed to light for 15 days. ....	41
Figure 19. Selected spectra of <i>Composition B Solution</i> treatments. ....	42
Figure 20. Solid state CP/MAS $^{13}\text{C}$ NMR of dry, solid RDX exposed to light for 15 days at 10-cm depth. ....	46
Figure 21. Solid state CP/MAS $^{15}\text{N}$ NMR spectra of $^{15}\text{N}$ -labeled TNT standard and unlabeled <i>Composition B</i> subjected to 15-day light exposure. ....	47
Figure 22. Liquid state $^{13}\text{C}$ NMR of dry, solid <i>Composition B</i> exposed to light for 15 days at 10-cm depth. ....	48

**Tables**

Table 1. Photochemical degradation products of TNT identified by Burlinson et al. (1979a). .....	2
Table 2. Photochemical degradation products of TNT identified by Spanggord et al. (1980) and Godejohann et al. (1998). .....	6
Table 3. Treatment summary. ....	9
Table 4. Mean ( $\pm$ standard deviation) light intensity and temperature at each distance from the light source. ....	16
Table 5. Assignments for NMR spectra of 1-hour T <sup>15</sup> N <sup>15</sup> photolysate, Figures 1 and 4. ....	21
Table 6. Peak areas as percent of total nitrogen for quantitative liquid state <sup>15</sup> N NMR spectrum of 1-hour T <sup>15</sup> N <sup>15</sup> photolysate. ....	24

## **Preface**

This report was prepared by the Environmental Laboratory (EL), U.S. Army Engineer Research and Development Center (ERDC), Vicksburg, MS; and the U.S. Geological Survey (USGS), Denver, CO. The research was sponsored by the Strategic Environmental Research and Development Program, Arlington, VA, Bradley P. Smith, Executive Director, and Dr. Jeff Marqusee, Technical Director, under Compliance Project Number CP-1155, now Environmental Restoration Project Number ER-1155. The principal investigator was Dr. Judith C. Pennington, Environmental Processes and Engineering Division (EPED), EL, ERDC. Co-principal investigators were Dr. Denise K. MacMillan, ERDC, and Dr. Kevin Thorn, USGS.

This report was reviewed by Dr. Anthony Bednar and Dr. Victor Medina, EL, ERDC. The study was conducted under the direct supervision of Dr. Richard E. Price, Chief, EPED, EL; and Dr. Beth Fleming, Director, EL, ERDC.

COL Richard B. Jenkins was Commander and Executive Director of ERDC. Dr. James R. Houston was Director.

## Acronyms

2ADNT	2-amino-4,6-dinitrotoluene
4ADNT	4-amino-2,6-dinitrotoluene
4,6-DNBA	4,6-dinitrobenzoic acid
4N2,4DAZB	4-nitro-2,4-diazabutanal
ADNBA	aminodinitrobenzoic acid
ADNT	aminodinitrotoluene
CP/MAS	cross polarization/magic angle spinning
DNAn	3,5-dinitroaniline
DNB	1,3-dinitrobenzene
DNBA	2,4-dinitrobenzoic acid
DOM	dissolved organic matter
HMX	octahydro-1,3,5,7-tetranitro-1,3,5,7-tetrazocine
LC-MS	liquid chromatography-mass spectrometry
LC-NMR	liquid chromatography-nuclear magnetic resonance
MNX	hexahydro-1-nitroso-3,5-dinitro-1,3,5-triazine
<i>m/z</i>	mass to charge ratio
NMR	nuclear magnetic resonance
NOM	natural organic matter



---

PFG	pulsed field gradient
RDX	1,3,5-trinitro-1,3,5-triazine
SRNOM	Suwannee River natural organic matter
TNB	1,3,5-trinitrobenzene
TNT	2,4,6-trinitrotoluene
TSP	Thermo Separation Products
UV	ultraviolet

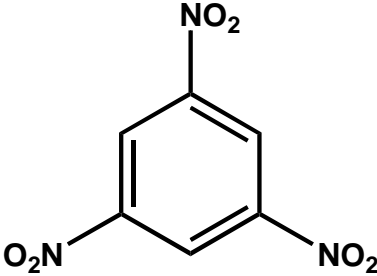
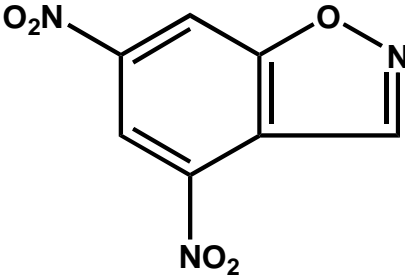
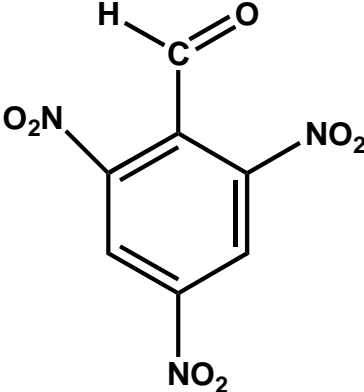
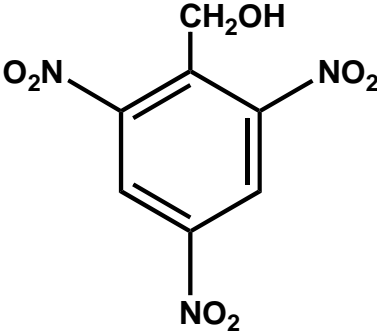
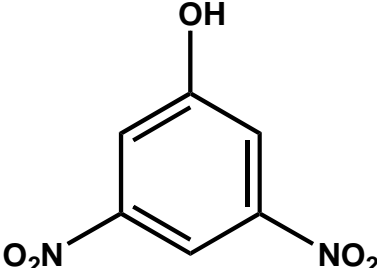
# 1 Introduction

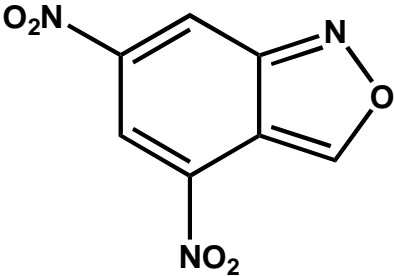
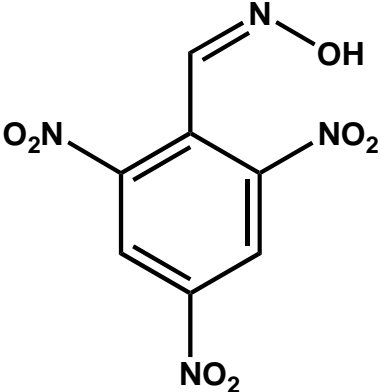
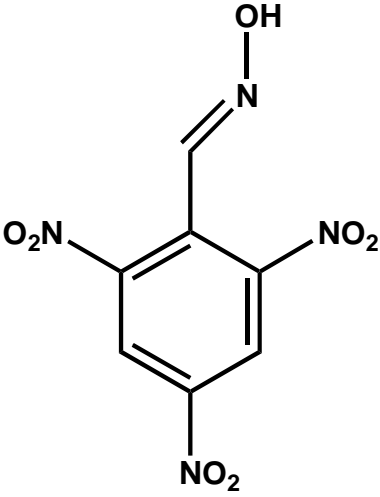
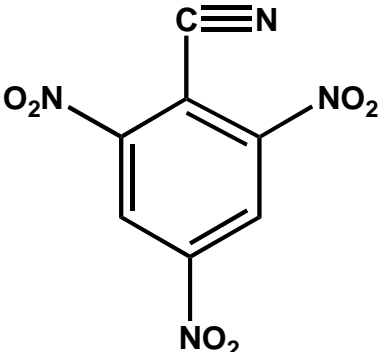
## Background

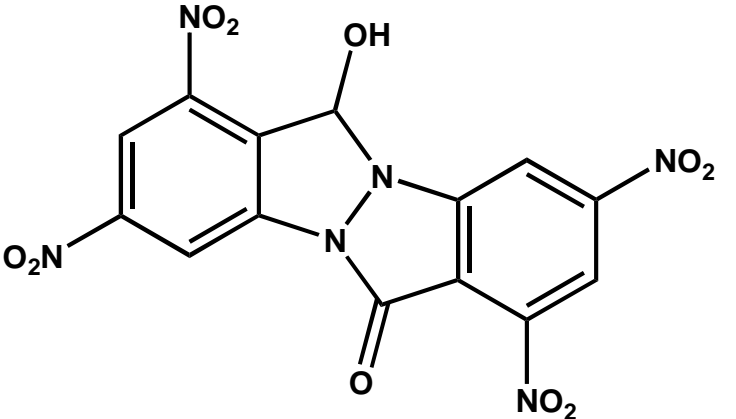
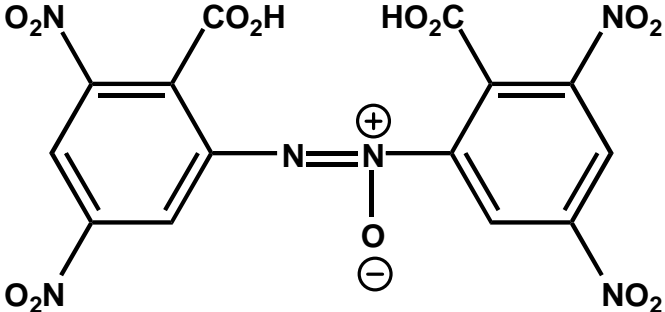
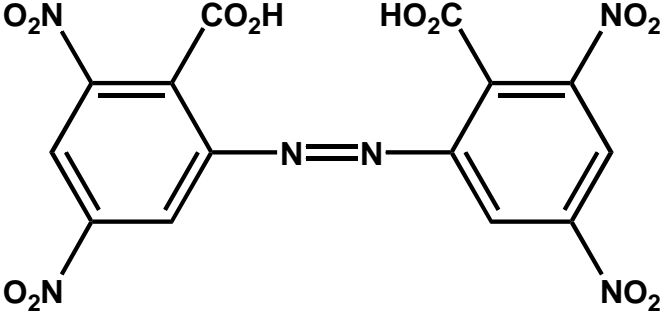
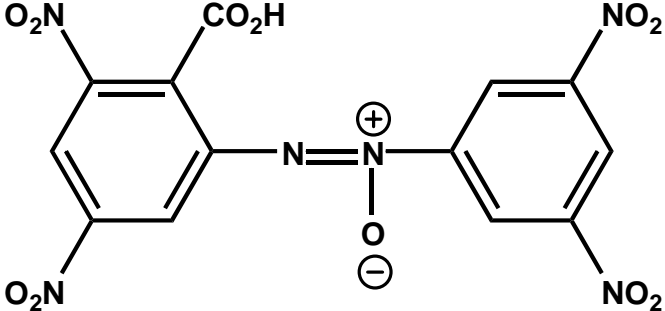
The photochemical transformation of 2,4,6-trinitrotoluene (TNT) has been previously investigated and reviewed (Burlinson et al. 1973; Kaplan et al. 1975; Burlinson et al. 1979a, 1979b; Spanggord et al. 1980; Rosenblatt et al. 1991; Godejohann et al. 1998; Talmage et al. 1999; Brannon and Pennington 2002; Lewis et al. 2004). Most of the research has been conducted in the aqueous phase. The most extensive studies on aqueous photolysis were conducted in the 1970s and 80s by Burlinson and Kaplan at the Naval Ordnance Laboratory, MD. They reported that 45 to 50 percent of the photodecomposition products of TNT were recovered in solution as 16 identifiable structures (Burlinson 1980; Burlinson et al. 1973, 1979a, 1979b; Kaplan et al. 1975). Several of these structures consisted of dimerization products of TNT. The remaining insoluble residues were not identified, but were postulated to consist of oligomers of azo or azoxy compounds. The effects of pH and the presence of dissolved organic matter (DOM), alternatively referred to as aquatic humic substances or natural organic matter (NOM), on the rates of TNT photolysis have also been investigated. Photochemical degradation was inversely proportional to pH over the range 1.1 to 11.1; however, these results were complicated by the fact that TNT undergoes alkaline hydrolysis at higher pH. Spanggord et al. (1980) and Mabey et al. (1983) noted that photolysis of TNT in river and pond water is more rapid than in distilled water. They both attributed the accelerated rates to the presence of NOM. Mabey et al. (1983) provided evidence that humic substances act as triplet sensitizers during aqueous photolysis of TNT in natural waters, and speculated that complexes (e.g., charge transfer) form between humic substances and TNT.

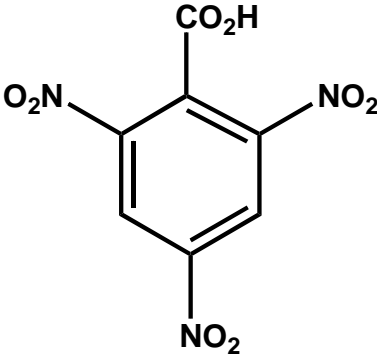
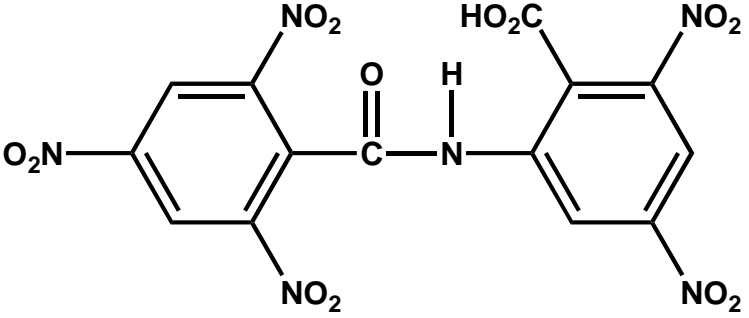
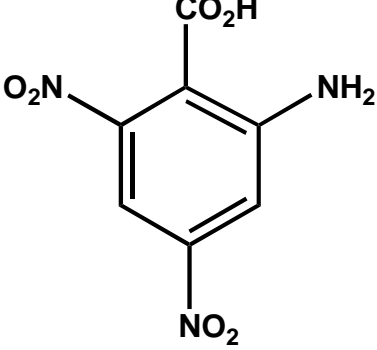
Table 1 lists degradation products identified by Burlinson (1979a) from ultraviolet (UV) irradiation of approximately 120 mg/kg TNT in distilled water using a medium pressure mercury lamp with a Pyrex filter. These degradation products were separated from the product mixture through solvent extraction followed by thin layer chromatography, and identified by a combination of mass spectrometry, infrared spectrometry, and  $^1\text{H}$  nuclear magnetic resonance (NMR) spectrometry. The remainder of the decomposition products consisted of an insoluble reddish brown residue. The components of the insoluble residue were not identified but were

Table 1. Photochemical degradation products of TNT identified by Burlinson et al. (1979a).

	Name	Structure
1	1,3,5-trinitrobenzene  0.5-1.0%  C <sub>6</sub> H <sub>3</sub> O <sub>6</sub> N <sub>3</sub> 213.1	
2	4,6-dinitroanthranil [4,6-dinitro-1,2-benzisoxazole]  3-4%  C <sub>7</sub> H <sub>3</sub> O <sub>5</sub> N <sub>3</sub> 209.1	
3	2,4,6-trinitrobenzaldehyde  8-10%  C <sub>7</sub> H <sub>3</sub> O <sub>7</sub> N <sub>3</sub> 241.1	
4	2,4,6-trinitrobenzyl alcohol  1%  C <sub>7</sub> H <sub>5</sub> O <sub>7</sub> N <sub>3</sub> 243.1	
5	3,5-dinitrophenol  1%  C <sub>6</sub> H <sub>4</sub> O <sub>5</sub> N <sub>2</sub> 184.1	

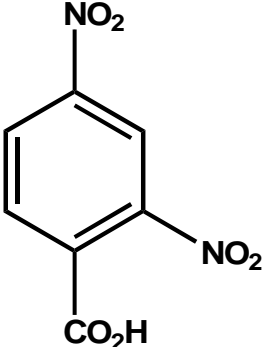
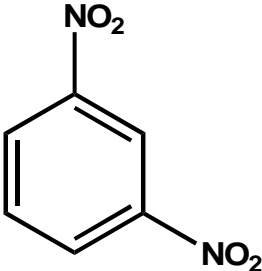
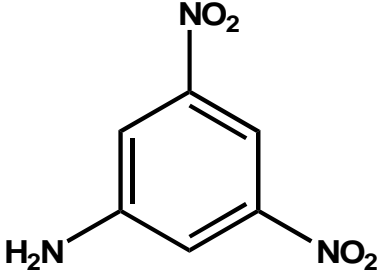
	Name	Structure
6	4,6-dinitroisoanthril [4,6-dinitro-2,1-benzisoxazole]  2%  C <sub>7</sub> H <sub>3</sub> O <sub>5</sub> N <sub>3</sub> 225.1	 <p>The structure shows a benzene ring fused to a five-membered isoxazole ring. The benzene ring has nitro groups (NO<sub>2</sub>) at the 4 and 6 positions relative to the fusion point.</p>
7	syn-2,4,6-trinitrobenzaldoxime  1%  C <sub>7</sub> H <sub>4</sub> O <sub>7</sub> N <sub>4</sub> 256.1	 <p>The structure shows a benzene ring with nitro groups (NO<sub>2</sub>) at the 2, 4, and 6 positions. An aldoxime group (-CH=N-OH) is attached to the benzene ring at the 1 position, with the hydroxyl group (OH) and the benzene ring on the same side of the C=N double bond.</p>
8	anti-2,4,6-trinitrobenzaldoxime  1%  C <sub>7</sub> H <sub>4</sub> O <sub>7</sub> N <sub>4</sub> 256.1	 <p>The structure shows a benzene ring with nitro groups (NO<sub>2</sub>) at the 2, 4, and 6 positions. An aldoxime group (-CH=N-OH) is attached to the benzene ring at the 1 position, with the hydroxyl group (OH) and the benzene ring on opposite sides of the C=N double bond.</p>
9	2,4,6-trinitrobenzotrile  3-4%  C <sub>7</sub> H <sub>2</sub> O <sub>6</sub> N <sub>4</sub> 238.1	 <p>The structure shows a benzene ring with nitro groups (NO<sub>2</sub>) at the 2, 4, and 6 positions. A nitrile group (-C≡N) is attached to the benzene ring at the 1 position.</p>

	Name	Structure
10	1,3,7,9-tetranitroindazolo-2,1-a-indazol-6-ol-12-one  1%	
11	2,2'-dicarboxy-3,3',5,5'-Tetranitroazoxybenzene  Trace %  $C_{14}H_6O_{13}N_6$ 466.2	
12	2,2'-dicarboxy-3,3',5,5'-Tetranitroazobenzene  7%  $C_{14}H_6O_{12}N_6$ 450.2	
13	2-carboxy-3,3',5,5'-tetranitro-NNO-azoxy benzene  2%  $C_{13}H_6O_{11}N_6$ 422.2	

	Name	Structure
14	2,4,6-trinitrobenzoic acid  1%  C <sub>7</sub> H <sub>3</sub> O <sub>8</sub> N <sub>3</sub> 257.1	
15	N-(2-carboxy-3,5-dinitrophenyl)-2,4,6-trinitrobenzamide  1%  C <sub>14</sub> H <sub>5</sub> O <sub>13</sub> N <sub>6</sub> 465.2	
16	2-amino-4,6-dinitrobenzoic acid  11%  C <sub>7</sub> H <sub>5</sub> O <sub>6</sub> N <sub>3</sub> 227.1	

postulated to consist of oligomers of azo or azoxy compounds. Other photodegradation compounds determined by Spangord et al. (1985) and Godejohann et al. (1998) include 2,4-dinitrobenzoic acid (2,4-DNBA), 1,3-dinitrobenzene (DNB), and 3,5-dinitroaniline (DNAn) (Table 2). Furthermore, 2-amino-4,6-dinitrobenzoic acid (2A4,6DNBA) and DNAn were detected in groundwater from a former ammunition site near Elsnig, Germany, using a combination of liquid chromatography-nuclear magnetic resonance (LC-NMR) and liquid chromatography-mass spectrometry (LC-MS) (Godejohann et al. 1998).

Table 2. Photochemical degradation products of TNT identified by Spanggord et al. (1980) and Godejohann et al. (1998).

	Name	Structure
A	2,4-dinitrobenzoic acid	
B	1,3-dinitrobenzene	
C	3,5-dinitroaniline	

Several studies have addressed the aqueous phase photolysis of RDX (1,3,5-trinitro-1,3,5-triazine) (Kubose and Hoffsomer 1977; Glover and Hoffsomer 1979; Spanggord et al. 1980; Peyton et al. 1999; Hawari et al. 2002; Just and Schnoor 2004). Photochemical degradation products reported from aqueous phase photolysis include formaldehyde, formic acid, formamide, ammonia, nitrite, nitrate, nitrous oxide, and 4-nitro-2,4-diazabutanal (4N2,4DAZB). In one instance, rates of photochemical degradation of solid RDX and octahydro-1,3,5,7-tetranitro-1,3,5,7-tetrazocine (HMX) in a potassium bromide matrix both in the presence of a medium pressure mercury lamp and in direct sunlight were reported (Bedford et al. 1996).

## Objectives

Products of photodecomposition of TNT have been observed as a coating on TNT particles and as a fine powdered residue surrounding TNT particles on ranges receiving limited rainfall and wind dispersion. For example photodegradation products of TNT, specifically 1,3,5-trinitrobenzene (TNB), DNB, and DNAn, were often detected in range soils during the execution of range characterization studies in Strategic Environmental Research and Development Program project ER-1155 (Pennington et al. 2001, 2002, 2003, 2004, 2005). The significance of photolysis on the composition of the source term of explosives contamination on ranges is unknown. In particular the effects of photolysis on explosive formulations, which are the form typically present on ranges, have not been described. Previous studies have not included the soil as a matrix for explosive particles. Therefore, photolysis of a common explosives formulation, Composition B, and its components in a soil matrix were included in this study. The objectives of the study were to:

- determine the rate of photolysis of TNT and RDX
- determine the effects of light intensity, duration, and moisture on photolysis rates in soils
- identify as many photolysis products as possible.

## Approach

Irradiation was performed in laboratory microcosms under controlled conditions. Irradiation of TNT solutions; TNT, Composition B, and RDX solids; and TNT, RDX, and Composition B in soils was conducted. Two approaches were used to characterize products of photodecomposition: LC/MS and a combination of solid and liquid state  $^{13}\text{C}$  and  $^{15}\text{N}$  NMR, and liquid state  $^1\text{H}$  NMR.

The LC/MS was used for specific characterization of photodecomposition products. The wide dynamic range of mass spectrometry permits observation of low abundance products in the presence of high concentrations (parts per million) of the parent compounds. Techniques to remove the parent compound would likely reduce the already low concentrations of products with similar structures and/or chemical properties and make their detection more difficult. In the absence of commercial standards, LC/MS provides the abundance of degradation products relative to parent compounds.



The entire product mixture from aqueous phase UV irradiation of TNT was analyzed by a combination of solid and liquid state  $^{13}\text{C}$  and  $^{15}\text{N}$  NMR, and liquid state  $^1\text{H}$  NMR. The objective was to determine the total distribution of carbon and nitrogen functional groups in the product mixture as a function of time. Additionally, a solvent fractionation procedure previously used by Burlinson et al. (1979a) was replicated on a solution of  $^{15}\text{N}$  labeled TNT irradiated for 1 hour and the fractions analyzed by NMR. The effect of naturally occurring DOM on the UV degradation of  $^{15}\text{N}$  labeled TNT was also examined. In these UV degradation experiments, a Pyrex filter, which eliminates radiation below 280 nm, was not used. Selected treatments of irradiated solid TNT, RDX, and Composition B and of irradiated solution TNT in soils were also analyzed by NMR.

## 2 Materials and Methods

### Irradiation

Various irradiation experiments were performed to generate photolytic products of TNT and RDX (Table 3). The Aqueous-Phase Irradiation treatments were analyzed by NMR only. All other treatments were analyzed by LC/MS. Selected Irradiation of Solids treatments and the *TNT Solution* tests in the Irradiation of Solutions in Soil treatments were analyzed by NMR as well as by LC/MS.

Table 3. Treatment summary.

Treatment Identifier	Source of Explosives	Matrix	Support	Humidity Added
<b>Aqueous-Phase Irradiation</b>				
<i>Aqueous-Phase Irradiations</i> <sup>1</sup>	T <sup>15</sup> NT and unlabelled TNT	Distilled Deionized Water	NA <sup>2</sup>	NA
<b>Irradiation of Solutions in Soil</b>				
<i>TNT Solution</i> <sup>1</sup>	100 mg/L Solution of Military grade TNT	Soil Slurry	Glass Plate	Yes
<i>Composition B Solution</i>	30 mg/L Solution of Solid Composition B Residue	Soil Slurry	Glass Plate	Yes
<b>Irradiation of Solids</b>				
<i>TNT Solids</i> <sup>1</sup>	Solid Military-Grade TNT	Moistened Filter Paper	Glass Dish	Yes
<i>RDX Solids</i> <sup>1</sup>	Solid Military-Grade RDX	Moistened Filter Paper	Glass Dish	Yes
<i>Composition B Solids</i> <sup>1</sup>	Solid Composition B Residue	Moistened Filter Paper	Glass Dish	Yes
<b>Irradiation of Solids in Soil, wet</b>				
<i>Wet TNT</i>	Solid Military Grade TNT Mixed with Wet Soil	Soil Slurry	Glass Plate	Yes
<i>Wet RDX</i>	Solid Military Grade RDX Mixed with Wet Soil	Soil Slurry	Glass Plate	Yes
<i>Wet Composition B</i>	Solid Composition B Residue Mixed with Wet Soil	Soil Slurry	Glass Plate	Yes
<b>Irradiation of Solids in Soil, dry</b>				
<i>Dry TNT</i>	Solid Military Grade TNT Mixed with Wet Soil	Soil Slurry	Glass Plate	No

<sup>1</sup> Samples analyzed by NMR as well as LC/MS.

<sup>2</sup> Not applicable.

**Aqueous-phase irradiations: T<sup>15</sup>NT and unlabeled TNT**

Unlabeled TNT, 99 percent purity, was purchased from Chem Service, Inc. (West Chester, PA). Labeled 2,4,6-trinitrotoluene-<sup>15</sup>N<sub>3</sub>, 99 atom percent <sup>15</sup>N, was purchased from ISOTECH (St. Louis, MO). Suwannee River Natural Organic Matter was purchased from the International Humic Substances Society (IHSS). Reagent grade diethyl ether was purchased from Aldrich (Dallas, TX). Reagent grade acetonitrile and toluene were purchased from Honeywell Burdick and Jackson (Morristown, NJ). The photochemical reactor (Ace Glass Inc., Vineland, NJ) consisted of a 450-watt, medium pressure, quartz, mercury-vapor lamp, housed in a quartz immersion well, and equipped with a 1.0-L reaction vessel. The Pyrex filter, which is typically used, was not used in these experiments. Two solutions of  $5 \times 10^{-4}$  M T<sup>15</sup>NT in distilled deionized water (100 mg in 900 mL H<sub>2</sub>O) were irradiated in the photochemical reactor for 1 and 16 hours, respectively. Additionally, solutions of unlabeled TNT were similarly irradiated for periods of 4 and 8 hours. The solutions were freeze dried until analyzed by NMR. For degradation in the presence of NOM, a solution of 340 mg Suwannee River natural organic matter (SRNOM) dissolved in 50 mL deionized water was added to a solution of 85 mg T<sup>15</sup>NT dissolved in 850 mL H<sub>2</sub>O. The solution was irradiated for 1 hour (final pH = 3.4) and then freeze dried.

**Aqueous-phase irradiations: Solvent fractionation of T<sup>15</sup>NT photolysate**

A separate solution of T<sup>15</sup>NT (95 mg in 850 mL deionized distilled water) was subjected to 1 hour of UV irradiation as described above. After irradiation, the pH of the solution was adjusted from pH 4.1 to  $\leq 2.0$  using 1N HCl. The aqueous solution was successively extracted with toluene and diethyl ether (ether I fraction). The pH of the aqueous phase was then adjusted to 1 with HCl and re-extracted with diethyl ether (ether II fraction). Material that precipitated out of the aqueous phase, but would not extract into toluene or ether, was dissolved into acetonitrile. NMR spectra were recorded on the toluene (5.7 mg yield), ether I (35 mg), and acetonitrile (17.8 mg) fractions.

**Irradiation of solution explosives in soils**

A surface soil containing 0.2 percent total organic carbon, 84 percent silt, 11 percent sand, and 5 percent clay (U.S. Department of Agriculture Natural Resources Conservation Service classification: Adler silt loam,

coarse-silty, mixed, superactive, thermic Fluvaquentic Eutrudepts) was air-dried, ground (Kelly Duplex industrial grinder, Springfield, OH) and sieved to  $\leq 2$  mm prior to use. Soils were amended with TNT and Composition B in solution. The Composition B was from mortar rounds that had been partially detonated in low-order detonation studies (Pennington et al. 2006, Chapter 9). The Composition B was in chunks of various sizes; therefore, the material was manually ground (mortar and pestle) and sieved to  $\leq 250$   $\mu\text{m}$ . Solutions were prepared in deionized, distilled water at  $100 \text{ mg L}^{-1}$  and  $30 \text{ mg L}^{-1}$  for TNT and Composition B, respectively. Each solution was added to the test soil in a 1:2.5 ratio of solution to soil. For each treatment the slurry was applied to triplicate 20-  $\times$  20-cm glass plates in a 1-mm film. After soil application, plates were air-dried overnight at room temperature in the dark. In order to maintain moisture at predetermined field capacity (moisture at 0.33 bar), weights of glass plates before and after application of the soil were used to determine the amount of moisture needed. Plates were misted with distilled deionized water and covered with thin polyethylene to aid in moisture retention. Treatments were irradiated by two 30-  $\times$  60-cm full spectrum light fixtures (American Environmental Products, Fort Collins, CO) mounted in a 60-  $\times$  60-  $\times$  122-cm wooden chamber. The chamber was fitted with three staggered, tiered shelves at distances of 10, 61, and 122 cm from the light source. Three plates (replicates) were placed on each shelf of the chamber. Ultraviolet light intensity was determined for each shelf using a Fisher-brand Traceable UV light meter (Fisher Scientific, Pittsburg, PA) with a wide-band wavelength of 320-390 nm. A PMA2100 data logger and PMA 2141 pyranometer (Solar Light Company, Philadelphia, PA) with a flat spectral response between 305-2800 nm provided broad spectrum light readings. All plates were kept at a moisture level of 0.33 bar. These treatments were designated *TNT Solution* and *Composition B Solution*, respectively. *Dark Controls* of each treatment were prepared in the same manner, but were stored in the dark. Plates were sampled at time 0, 1, 3, 7, and 15 days by scraping a 2.54-cm (1 in.) strip of soil from the length of each plate, transferring the sample to an amber glass vial and refrigerating until prepared for analyzed.

The *TNT Solution* samples were also analyzed by NMR. Only replicates exposed for the longest time (15 days) at the closest distance to the lamp (10 cm) were selected based upon the assumption that these samples would contain the largest concentration of photochemical degradation products. A solid state cross polarization/magic angle spinning (CP/MAS)

$^{13}\text{C}$  NMR spectrum was recorded on the soil before extraction to determine whether resonances attributable to TNT or TNT degradation products could be resolved from the broad peaks representing the NOM in the soil. Once this was completed, the soil was Soxhlet extracted with acetonitrile for 93 hours. The acetonitrile was removed with a rotary evaporator and the residue redissolved in dimethyl- $^{12}\text{C}_2$ , D6-sulfoxide for liquid state  $^{13}\text{C}$  NMR analysis.

### **Irradiation of solids**

Military grade crystalline compounds TNT and RDX were used as received from the manufacturer (Holston Army Ammunition Plant, Kingsport, TN). Nine Petri dishes (three replicates per explosives compound) containing four 0.15-gram samples of either TNT, RDX, or Composition B on separate quadrants of moist filter paper were placed on each shelf. Moisture was maintained throughout the experiment by consistently wetting the filter paper with distilled deionized water and covering the Petri dishes with a thin layer of polyethylene plastic. One 0.15-gram sample for each test compound was removed at 1, 3, 7, and 15 days, placed in an amber vial and refrigerated until analyzed by LC/MS. Treatments were designated *TNT Solid*, *RDX Solid*, and *Composition B Solid*, respectively. Subsamples from the three replicates of the *TNT Solids* treatment were combined for solid state  $^{13}\text{C}$  and  $^{15}\text{N}$  CP/MAS NMR spectral analysis. Subsamples from the three replicates of the *RDX Solids* treatment were combined for solid state  $^{13}\text{C}$  CP/MS spectral analysis. Subsamples from the three replicates of the *Composition B Solids* treatment were combined for solid state  $^{15}\text{N}$  CP/MAS and liquid state  $^{13}\text{C}$  NMR spectral analysis.

### **Irradiation of solid explosives in soils, wet and dry**

Solid TNT and Composition B were mixed with separate aliquots of dry soil in a 1:6 explosive to soil ratio. The mixture was moistened (1:2.5 distilled deionized water to soil mixture) to facilitate application to 20- × 20-cm glass plates in a 1-mm film. After soil application, plates were air-dried overnight at room temperature in the dark. One set (three replicates for each distance from the light source) of TNT plates were kept dry throughout the experiment (designated *Dry TNT*), but a second set of TNT plates and a set of both RDX and Composition B plates were kept moist to predetermined field capacity. These were designated *Wet TNT*, *Wet RDX*, and *Wet Composition B*, respectively. Three control plates of each treatment, except for the *Solids* treatments, were kept in the dark (designated

*Dark Controls*). *Dark Controls* for the TNT and RDX solids (two replicates) were drawn from the solid stock of each compound stored in amber bottles. The dark control for Composition B (two replicates) was drawn from the ground and sieved stock, which was also stored in amber bottles. Light intensity and temperature were measured at each distance from the light source. Plates were sampled at time 0, 1, 3, 7, and 15 days as described for "Irradiation of solution explosives in soils." Samples were stored in amber vials until analyzed.

### **Liquid chromatograph/mass spectrometry analysis of soils and solids**

Approximately 1-g soil from each replicate was diluted with high performance liquid chromatography (HPLC) grade acetonitrile and extracted overnight in a water-cooled sonicator (temperature was not monitored). The extract was allowed to settle and was filtered through a 0.45- $\mu\text{m}$  syringe filter directly into an amber autosampler vial. Extracts were stored at 4 °C prior to analysis. The solid materials were diluted with 1-2 mL acetonitrile prior to analysis. Sample extracts and diluted solids were analyzed on a Thermo Finnigan TSQ Quantum Discovery Max triple quadrupole mass spectrometer (Thermo Fisher Scientific, Inc., Waltham, MA) equipped with an electrospray source and liquid chromatography system. Sample injection volume was 1  $\mu\text{L}$ . Sample components were separated by using a Phenomenex Ultracarb 5  $\mu\text{m}$  ODS (30) 150  $\times$  1.00 mm chromatography column (Thermo Fisher Scientific, Inc.). The system used Thermo Surveyor pumps and Thermo Separation Products (TSP) UV6000 UV detector monitored at 254 nm. The flow rate was 0.1 mL/min. The samples were eluted with a gradient of 45 percent methanol:55 percent 40 mM ammonium acetate to 65 percent methanol:35 percent 40 mM ammonium acetate over 20 min, then to 100 percent methanol over 15 min, and held at 100 percent methanol for 35 min to clean the column and prevent carry-over into the next sample in the analytical sequence. The system was allowed to equilibrate prior to each sample injection. The TSQ mass spectrometer was operated in full scan mode. The electrospray voltage was 4 kilovolts and the capillary temperature was set to 180 °C. Spectra were collected in negative ion mode due to the high electron affinity of explosives compounds. Some explosives compounds were observed as anions generated by loss of a hydrogen atom and are represented as (M-H)<sup>-</sup> where M refers to the intact molecular species. Other explosives compounds were observed as anions generated by addition of an acetate species from the mobile phase and loss of a hydrogen atom. These adduct anions are

represented here as (M+Ac-H)<sup>-</sup>, where M is again the molecular species and Ac refers to acetic acid.

Selected ion current profiles for masses corresponding to known or suggested photolysis products were plotted for each sample. Also, selected ion profiles were acquired for ions with peak areas exceeding 10<sup>5</sup> ion counts. Relative ion abundances were obtained by comparing the selected peak areas to the peak area observed for the parent compound. For each profiled ion, the observed relative abundance was compared to the observed relative abundance for the corresponding ion, if present, in the appropriate control. Ion signal abundances (i.e., abundances relative to the ion signal abundances of RDX or TNT present in the same sample) were plotted against sample exposure time and distance to the light sources to evaluate trends.

## Nuclear magnetic resonance spectrometry

Solid state NMR spectra were recorded on the freeze dried powders from the aqueous phase irradiation for photochemical degradation procedure. Liquid state NMR spectra were recorded on the powders dissolved in dimethyl-<sup>12</sup>C<sub>2</sub>,d<sub>6</sub> sulfoxide (99.9 atom percent <sup>12</sup>C).

Solid state CP/MAS <sup>15</sup>N and <sup>13</sup>C NMR spectra were generated using a Chemagnetics CMX-200 NMR spectrometer at nitrogen and carbon resonant frequencies of 20.3 and 50.3 MHz, respectively, using a 7.5 mm ceramic probe (zirconium pencil rotors). Acquisition parameters for <sup>15</sup>N included a 26666.7-Hz spectral window, 19.201-ms acquisition time, 2.0-ms contact time, 0.5-s pulse delay, and spinning rate of 5 KHz. Nitrogen-15 chemical shifts were referenced to glycine, taken as 32.6 ppm<sup>1</sup>. Acquisition parameters for <sup>13</sup>C included a 30,030.0-Hz spectral window, 17.051-ms acquisition time, 2.0-ms contact time, 1.0-s pulse delay, and spinning rate of 5 KHz.

Liquid phase NMR spectra of the unfractionated photolysates were recorded on a GEMINI 2000 NMR spectrometer (Varian, Inc., Palo Alto, CA) at proton, carbon, and nitrogen resonant frequencies of 300.0, 75.4, and 30.4 MHz, respectively. Spectra of unfractionated photolysates were

---

<sup>1</sup> The ppm designation in the NMR context throughout this chapter is the standard unit for the chemical shift position in NMR. It refers to the resonance frequency in Hertz at which a nucleus absorbs radiation and is not to be confused with parts-per-million concentration units used elsewhere in this report.

recorded on a 10 mm broadband probe,  $^{13}\text{C}$  and  $^{15}\text{N}$  spectra of the solvent fractions on a 5 mm broadband probe, and  $^1\text{H}$  spectra of the solvent fractions on a 5 mm PFG (pulsed field gradient) indirect detection probe. Acquisition parameters for  $^1\text{H}$  NMR spectra included an 8,000-Hz spectral window, 45 deg pulse angle, 2.5-s acquisition time, and 1-s pulse delay. Acquisition parameters for  $^{13}\text{C}$  NMR spectra included a 30,000-Hz spectral window, 45 deg pulse angle, 0.5-s acquisition time, 1.0-s pulse delay, and continuous decoupling. Acquisition parameters for  $^{15}\text{N}$  NMR spectra included a 35,112-Hz spectral window, 45 deg pulse angle, 0.2-s acquisition time, 2.0-s pulse delay, and inverse gated decoupling (Figures 4, 5, and 13 in next chapter). Acquisition parameters for ACOUSTIC  $^{15}\text{N}$  NMR spectra included a 35,112 Hz spectral window, 0.2-s acquisition time, 0.25-s pulse delay, and tau delay of 0.1-msec (Figure 12 in next chapter).



### 3 Results

Ultraviolet light intensity decreased by approximately one order of magnitude from the top to the bottom shelf of the light chamber (Table 4). The mean ambient temperature for all treatments, distances from the light source, and sampling times was  $23 \pm 2.0$  °C. However, the shelf closest to the light source ( $25 \pm 2.2$  °C) was significantly warmer (Kruskal-Wallis One Way analysis of Variance on Ranks,  $P \leq 0.001$ ) than the shelves at 61 cm ( $23.4 \pm 1.9$  °C) and 122 cm ( $23.4 \pm 1.8$  °C), respectively, probably due to heat from the light.

Table 4. Mean ( $\pm$  standard deviation) light intensity and temperature at each distance from the light source. N was 35 (7 treatments and 5 sampling times at each distance).

Distance cm	UV Intensity <sup>1</sup> mW/cm <sup>2</sup>	Broad Spectrum Intensity <sup>2</sup> mW/cm <sup>2</sup>	Temperature °C
10	0.020 (0.0031)a	2.7 (0.36)a	25.19 (0.779)a
61	0.0082 (0.00062)b	1.0 (0.19)b	23.36 (0.663)b
122	0.0023 (0.00046)c	0.30 (0.098)c	23.38 (0.647)b

<sup>1</sup> Ultraviolet intensity was within the 320 to 390 nm range. Units are milliwatts per square centimeter. Lower case letters in each column indicate significant differences at the  $P = <0.001$  level (Kruskal-Wallis one way analysis of variance on ranks followed by Dunn's Pairwise Multiple Comparison Procedure).

<sup>2</sup> Light intensity was in the range of 305 to 2,800 nm.

### Aqueous-phase irradiation

#### NMR spectra of photolysates

Liquid and solid state <sup>13</sup>C and <sup>15</sup>N NMR spectra of the 1-hour T<sup>15</sup>NT photolysate are shown in Figures 1–4. In general, whereas the solid state CP/MAS measurement provides a greater signal to noise ratio per unit of spectrometer time, liquid state analysis provides greater resolution and the potential for quantitative accuracy. Both sets of measurements provide complementary information in this study. The spectra represent the distribution of carbon and nitrogen nuclei in the entire product mixture. One of the outstanding features of the spectra is the lack of sharp peaks. The product mixture can be assumed to comprise the structures listed in Tables 1 and 2 in addition to the uncharacterized, insoluble residue

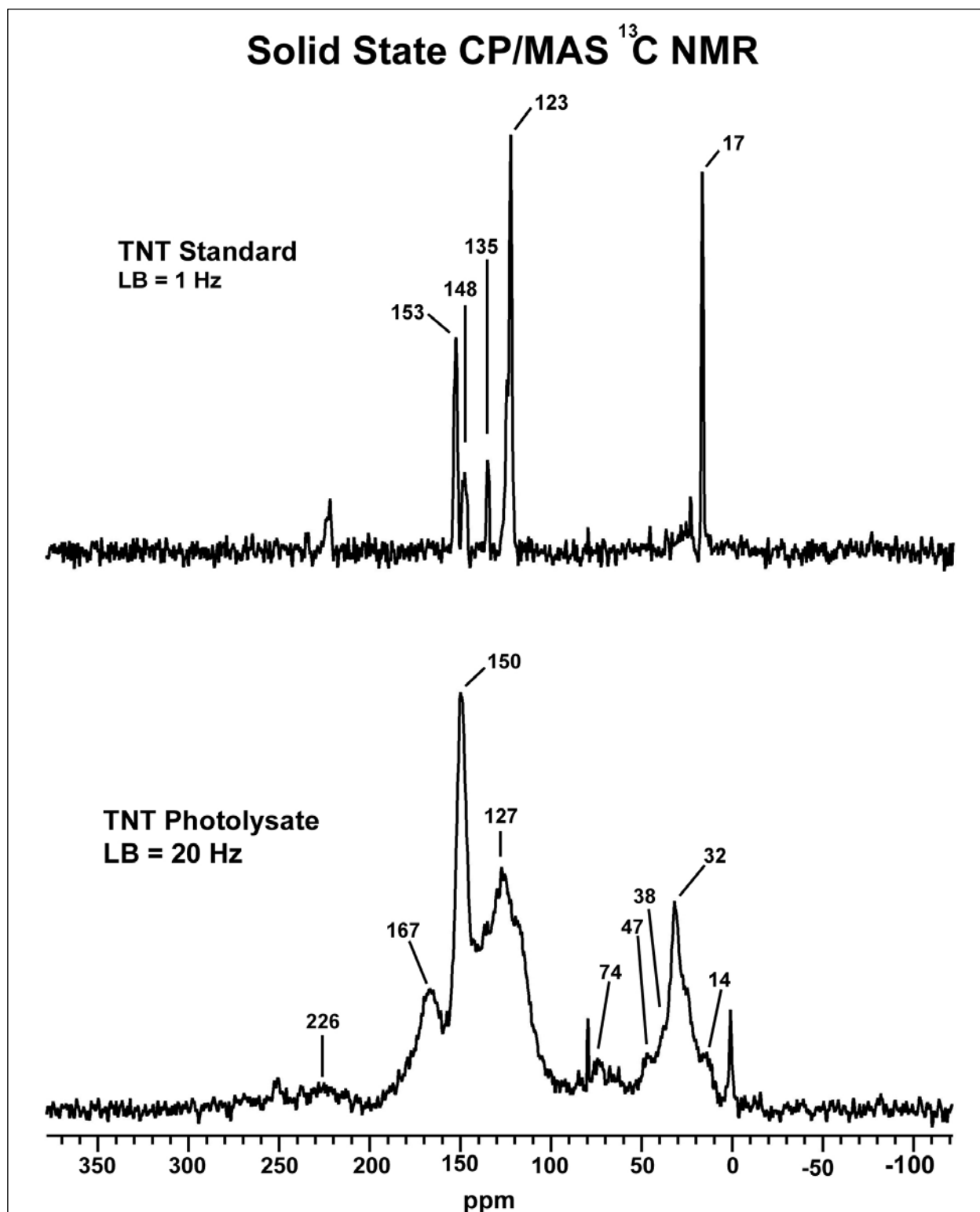


Figure 1. Solid state CP/MAS  $^{13}\text{C}$  NMR spectrum of 1-hour  $\text{T}^{15}\text{NT}$  photolysate.

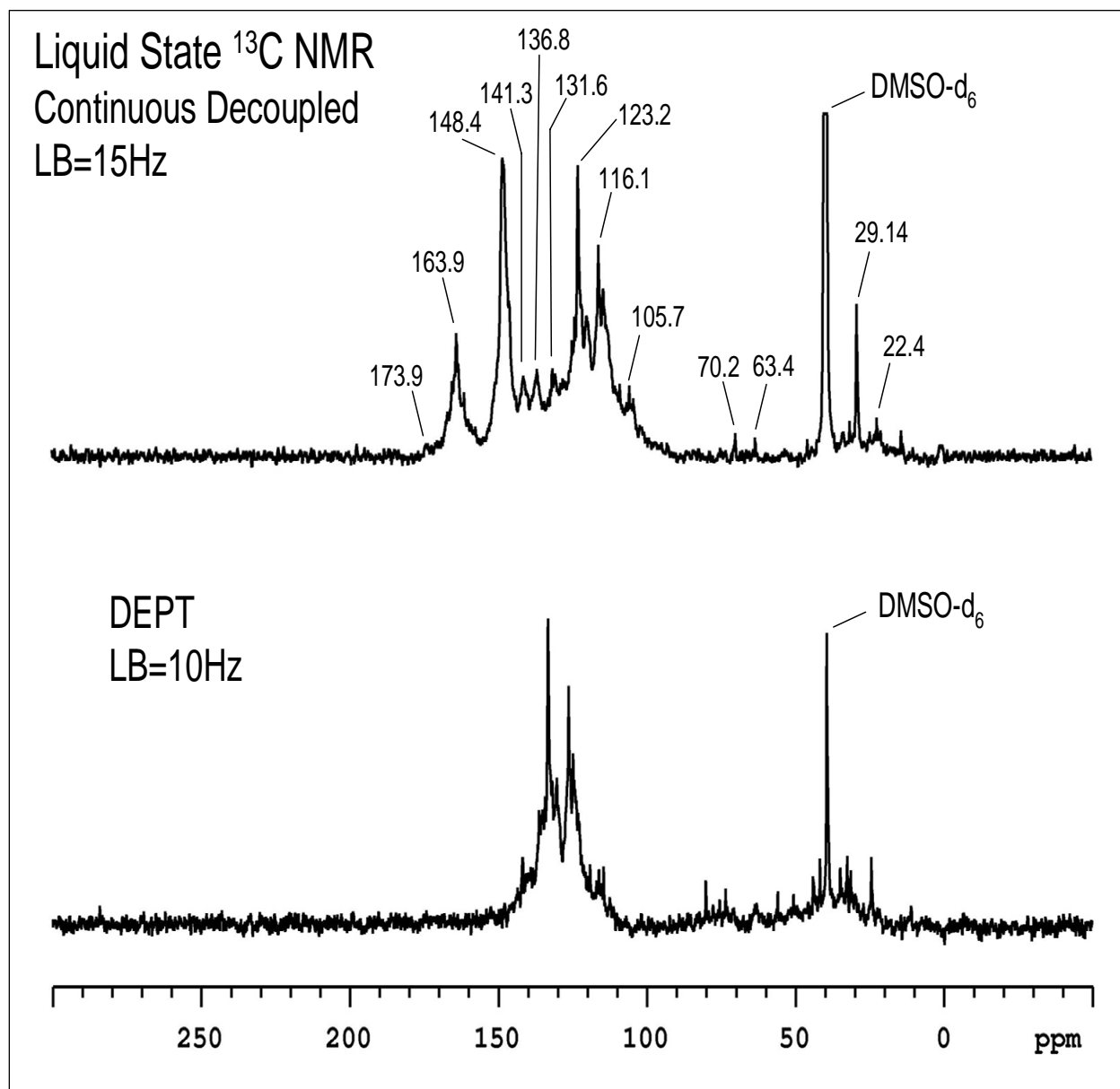


Figure 2. Continuous decoupled liquid state  $^{13}\text{C}$  NMR spectra of 1-hour  $\text{T}^{15}\text{NT}$  photolysate.

described by Burlinson et al. (1979a). The fact that the spectra exhibit broad bands suggests that the number of constituents in the insoluble residue may be an order of magnitude or greater than the 16 constituents identified, and that the insoluble residue may indeed be comprised of oligomeric or polymeric condensation products of the TNT. Otherwise, sharp peaks corresponding to the identified structures would be visible. It is also possible that exposure to irradiation below 280 nm resulted in a greater number of degradation products compared to the experimental conditions employed by Burlinson.

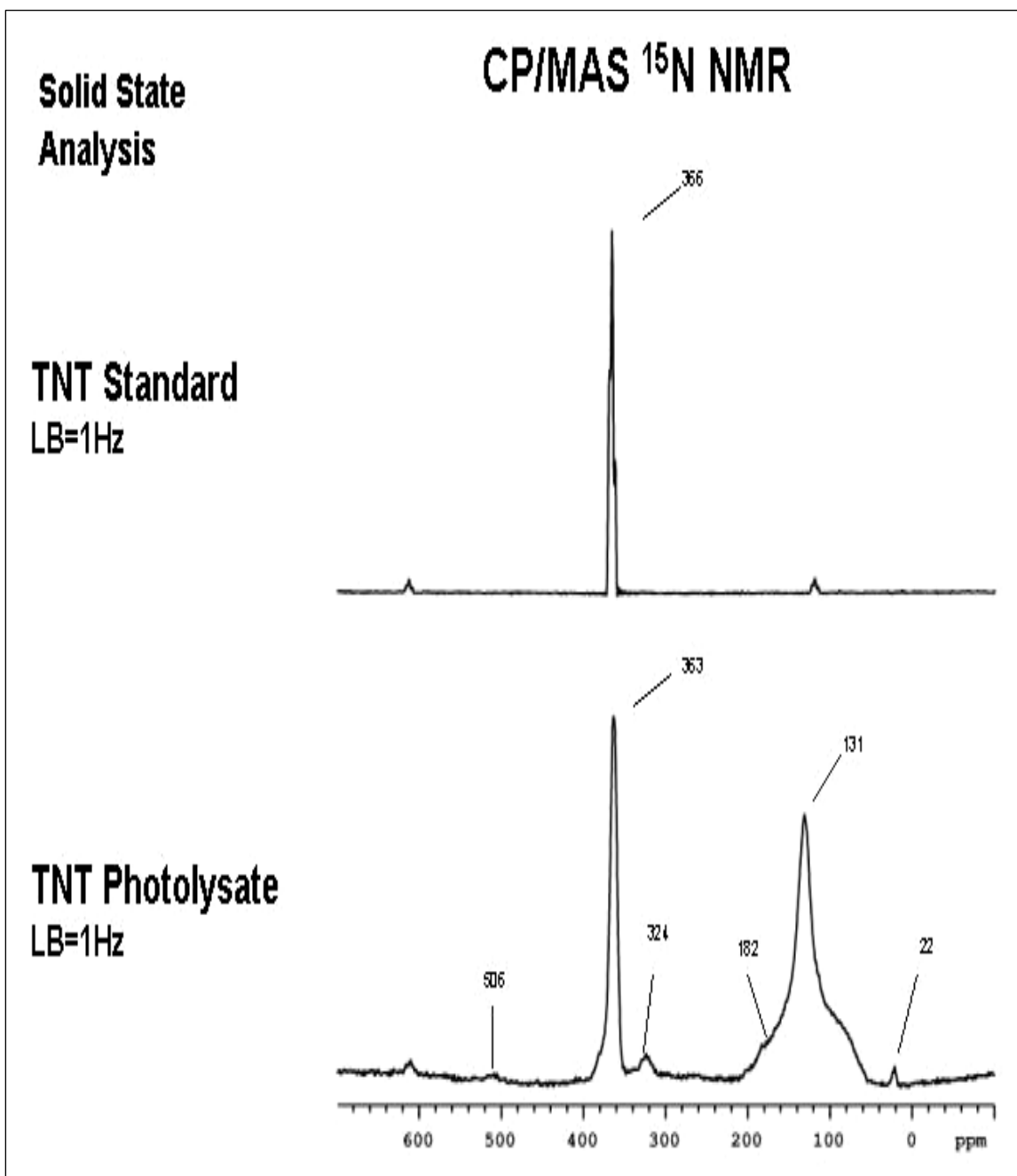


Figure 3. Solid state CP/MAS  $^{15}\text{N}$  NMR spectrum of 1-hour  $\text{T}^{15}\text{NT}$  photolysate.

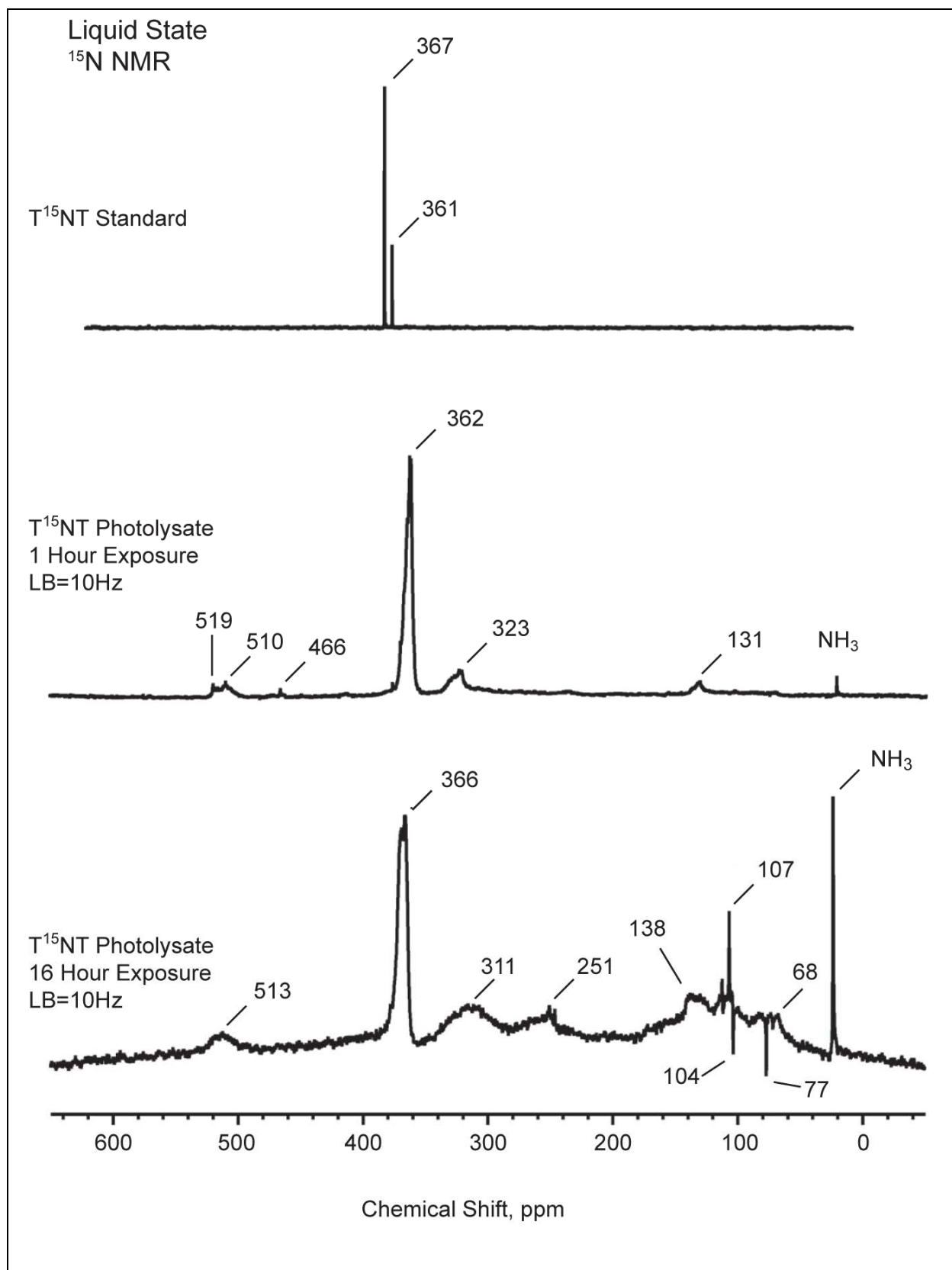


Figure 4. Quantitative inverse gated decoupled liquid state  $^{15}\text{N}$  NMR spectra of  $\text{T}^{15}\text{NT}$  standard, 1-hour photolysate, and 16-hour photolysate.

The solid state  $^{13}\text{C}$  NMR spectra of the parent TNT and the 1-hour  $\text{T}^{15}\text{NT}$  photolysate are compared in Figure 1. Assignments for the carbon atoms of the parent TNT are:  $\text{C}_1 = 135$  ppm;  $\text{C}_2$  and  $6 = 153$  ppm;  $\text{C}_4 = 148$  ppm;  $\text{C}_3$  and  $5 = 123$  ppm; methyl = 17 ppm. The spectrum of the photolysate indicates formation of aliphatic carbons at 32, 38, and 47 ppm, alcohol carbons at 74 ppm, carboxyl and amide carbons at 167 ppm, and ketone carbons at 226 ppm. Assignments for the major peaks in the spectrum are listed in Table 5, along with the structures identified by Burlinson that correlate with the peaks. Some peaks in the spectrum do not correlate with any of the structures identified by Burlinson, such as the aliphatic methylene carbons at 32 ppm. The liquid state  $^{13}\text{C}$  NMR spectrum (continuous decoupled, nonquantitative) of the 1-hour photolysate in Figure 2 shows additional detail in the aromatic region, with resolved peaks at 141.3, 136.8, 131.6, 123.2, 116.1, and 105.7 ppm.

Table 5. Assignments for NMR spectra of 1-hour  $\text{T}^{15}\text{NT}$  photolysate, Figures 1 and 4.

$^{13}\text{C}$ Peak <sup>1</sup> (Figure 1)	Functional Group	Structure Corresponding to Numbered Structures in Table 1
226 ppm	Benzaldehyde	3
167 ppm	Carboxylic acid	11-16
167 ppm	Amide	10, 15
150 ppm	Aldoxime	7, 8
127 ppm	Nitrile	9
74 ppm	benzyl alcohol	4
74 ppm	tertiary alcohol	10
47 ppm	Diphenyl methylene	
32 ppm	Methylene	
<b><math>^{15}\text{N}</math> Peak <sup>2</sup> (Figure 4)</b>		
519, 510 ppm	Azobenzene	12
466 ppm	azo-hydrazone	
362 ppm	nitro	
362 ppm	aldoxime	7, 8
362 ppm	benzoxazole	2, 6
323 ppm	azoxy	11, 13
235 ppm	nitrile	
131 ppm	amide	10, 15
71 ppm	aromatic amine	16, C
22 ppm	ammonia	

<sup>1</sup> Peak assignments for solid state spectrum

<sup>2</sup> Peak assignments for liquid state spectrum.

The solid state CP/MAS  $^{15}\text{N}$  NMR spectrum of the 1-hour  $\text{T}^{15}\text{NT}$  photolysate is compared with the  $\text{T}^{15}\text{NT}$  standard in Figure 3. The nitro groups of the standard occur at 366 ppm. Residual nitro groups in the photolysate occur at 363 ppm. Numerous other peaks in the spectrum confirm photochemical transformation of the nitro groups into other nitrogen functionalities. Because the liquid state spectrum is more clearly resolved, attention is focused on it (Figures 4 and 5). The fact that the spectrum is comprised of broad bands is further confirmation of the complexity of the product mixture. Some of the notable features are the ammonia peak at 22 ppm, amide peak at 131 ppm, nitrile peak at 235 ppm, azoxy peak at 323 ppm, and azo peaks at 519 and 510 ppm. The spectrum represents the quantitative distribution of nitrogens in the product mixture. The spectrum is consistent with the results of Burlinson et al. (1979a) in that azoxy and azo compounds are major components of the product mixture. Table 5 summarizes assignments. Structures identified by Burlinson that correlate to the individual peaks are noted. Table 6 lists peak areas of the liquid state spectrum of the 1-hour photolysate.

Solid state  $^{13}\text{C}$  CP/MAS spectra of 1-, 4-, 8-, and 16-hour photolysates are compared in Figure 6. As the time of exposure increases, the proportion of carboxylic acid groups increases (peaks centered at 161-169 ppm), aliphatic alcohol carbons increase (peak at 63 ppm), and methyl carbons (peak at 17 ppm in standard) are converted to methylene, alcohol, and carboxylic acid carbons. The aromatic carbon in the number 4 position of TNT ( $\text{C}_4 = 148$  ppm) appears to be most resistant to chemical alteration, as the peak at 148 ppm persists through the 16 hours of irradiation.

Continuous decoupled liquid state  $^{13}\text{C}$  NMR spectra of the 1- and 16-hour  $\text{T}^{15}\text{NT}$  photolysates are compared in Figure 7. The 16-hour photolysate exhibited less structural detail than the 1-hour photolysate. For example, the peak at 123 ppm in the 1-hour photolysate, corresponding to carbons that originate from the  $\text{C}_3$  and  $\text{C}_5$  positions of the TNT, is significantly reduced in intensity in the 16-hour photolysate.

Liquid state inverse gated decoupled  $^{15}\text{N}$  NMR spectra (quantitative) of the 1- and 16-hour photolysates of  $\text{T}^{15}\text{NT}$  are compared in Figures 4 and 5. In the 1-hour photolysate, the ratio of nitro groups to other nitrogens is greater than in the 16-hour photolysate, indicating that nitro groups continue to be lost as the irradiation proceeds from 1 to 16 hours. In the spectrum of the 16-hour photolysate, peaks that can be attributed to

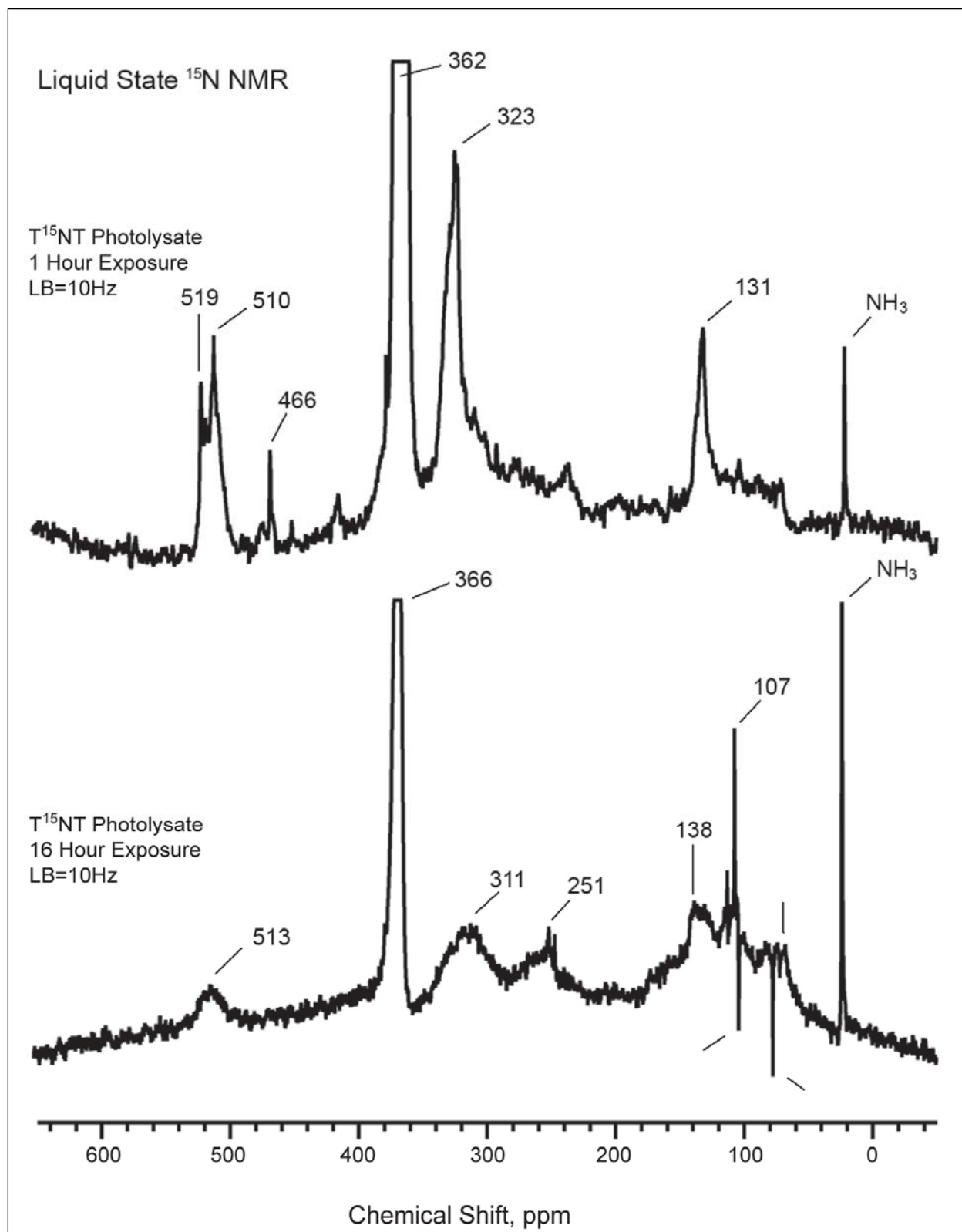


Figure 5. Vertical scale expansions of quantitative inverse gated decoupled liquid state  $^{15}\text{N}$  NMR spectra of 1- and 16-hour  $\text{T}^{15}\text{NT}$  photolysates.



Table 6. Peak areas as percent of total nitrogen for quantitative liquid state  $^{15}\text{N}$  NMR spectrum of 1-hour  $\text{T}^{15}\text{NT}$  photolysate.

Chem Shift Range ppm	Peak Maxima ppm	Assignment	Percent
600-490	519,510	Azo	5.4
490-448	466	Azo-hydrazone	0.5
448-413	414	Furazan, nitrosophenol	0.9
413-352	362	Nitro, aldoxime, benzisoxazole	57.7
352-289	323	Azoxy, imine	18.4
289-224	235	Nitrile Imine, imidazole	6.4
224-125	131	Amide	7.8
125-66	104,71	Amine	3.4
66-0	22	Ammonia <sup>1</sup>	

<sup>1</sup> Ammonia peak not integrated.

azobenzene nitrogens (513 ppm), nitro groups (366 ppm), azoxy and imine nitrogens (311 ppm), nitrile nitrogens (251 ppm), amide nitrogens (138 ppm), aromatic amine nitrogen (~125-66 ppm), and ammonia (22 ppm), are still present.

### Spectra of solvent fractionated $\text{T}^{15}\text{NT}$ solvent

Liquid state  $^1\text{H}$  (Figures 8-11) and  $^{15}\text{N}$  (Figure 12) NMR spectra were recorded on the ether I and acetonitrile fractions; a proton spectrum was also recorded on the toluene fraction. The acetonitrile fraction is presumed to correspond to the “insoluble residue” described by Burlinson et al. (1979a). The proton spectra (Figure 8) revealed numerous sharp peaks that may be correlated to identifiable compounds upon further analysis. The aromatic protons in position 3 and 5 of the parent TNT occur at 9.0 ppm. In the  $^1\text{H}$  NMR spectra of the solvent fractions of the photolysate, the range of aromatic protons occurs from ~7.0 to 9.6 ppm. This reflected the change of substitution patterns in the aromatic rings of the photo-degradation products. Protons bonded to the amide nitrogens visible in the  $^{15}\text{N}$  NMR spectra from 130-135 ppm would occur in the  $^1\text{H}$  NMR

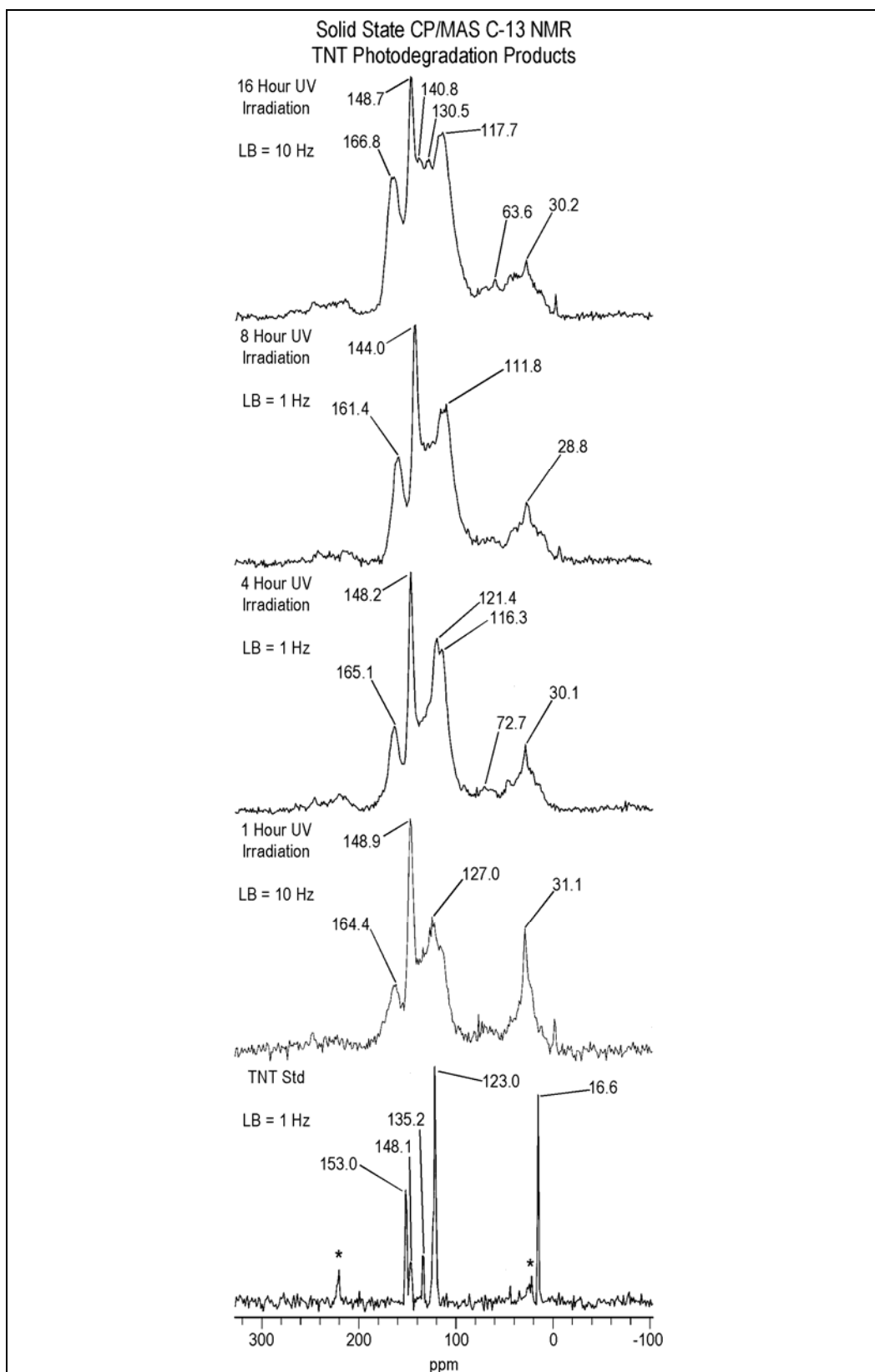


Figure 6. Solid state CP/MAS  $^{13}\text{C}$  NMR spectra of 1-, 4-, 8-, and 16-hour TNT photolysates and TNT standard.

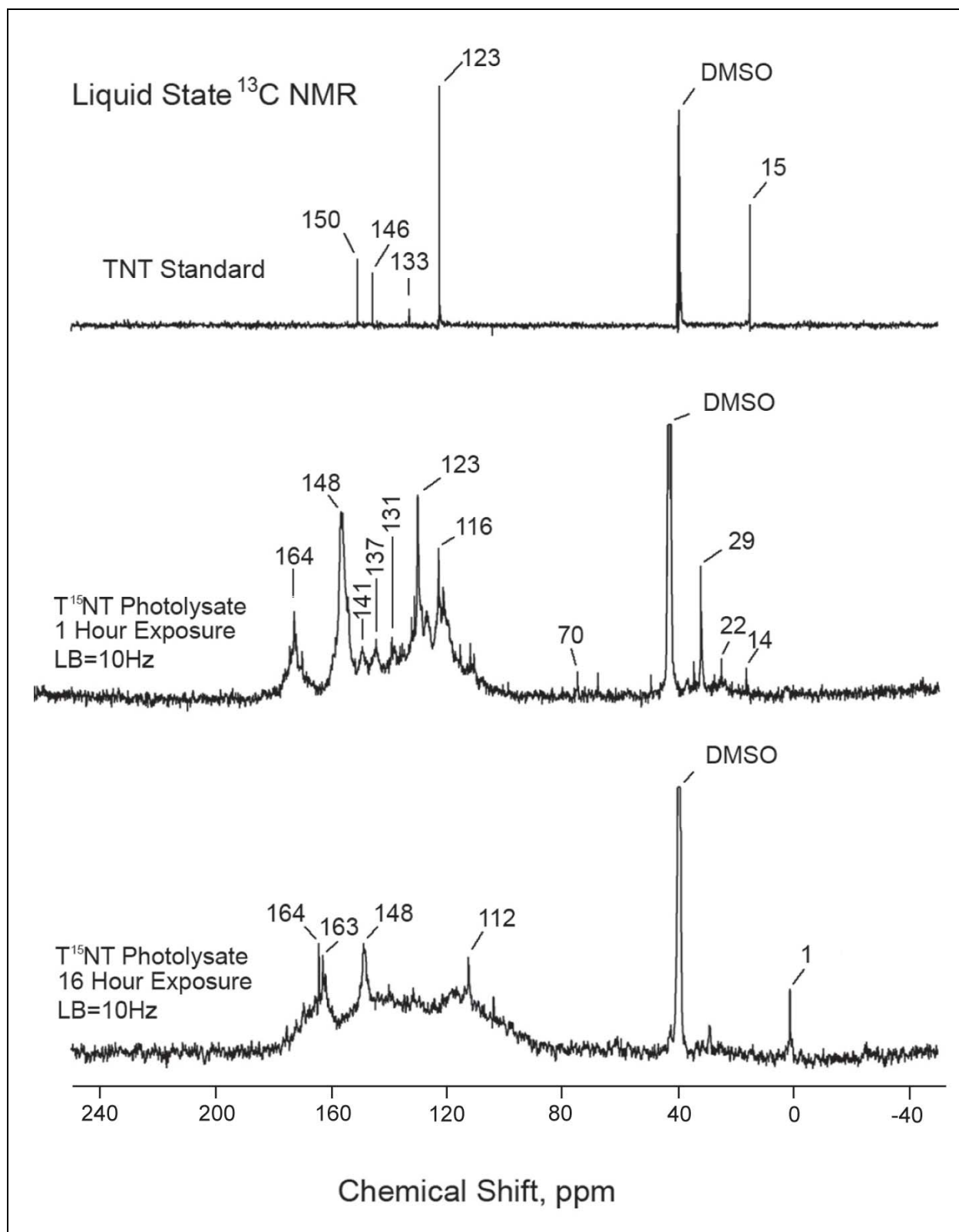


Figure 7. Continuous decoupled liquid state  $^{13}\text{C}$  NMR spectra of 1- and 16-hour  $\text{T}^{15}\text{NT}$  photolysates.

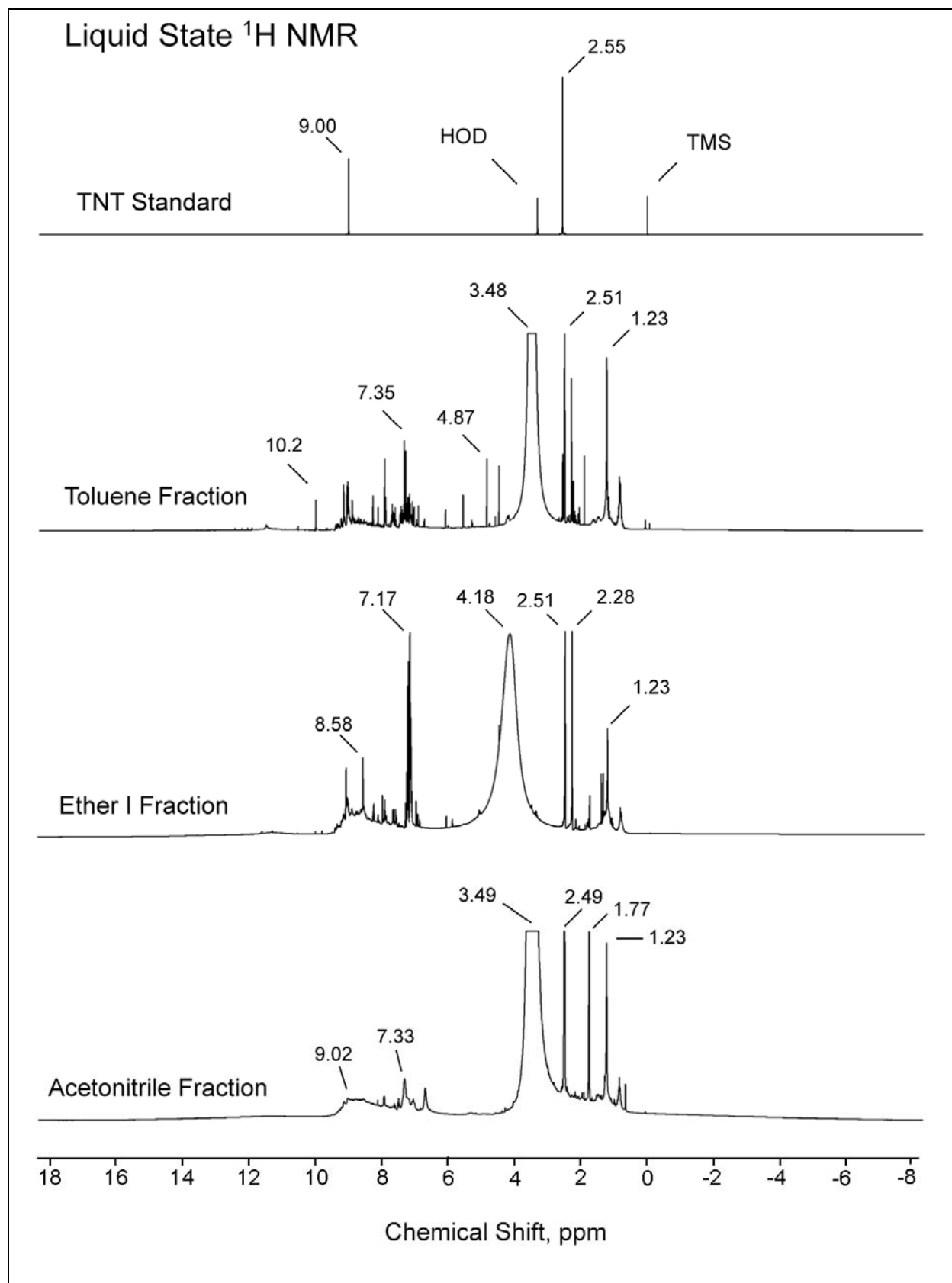


Figure 8. Liquid state  $^1\text{H}$  NMR spectra of solvent fractionated 1-hour  $\text{T}^{15}\text{NT}$  photolysate.

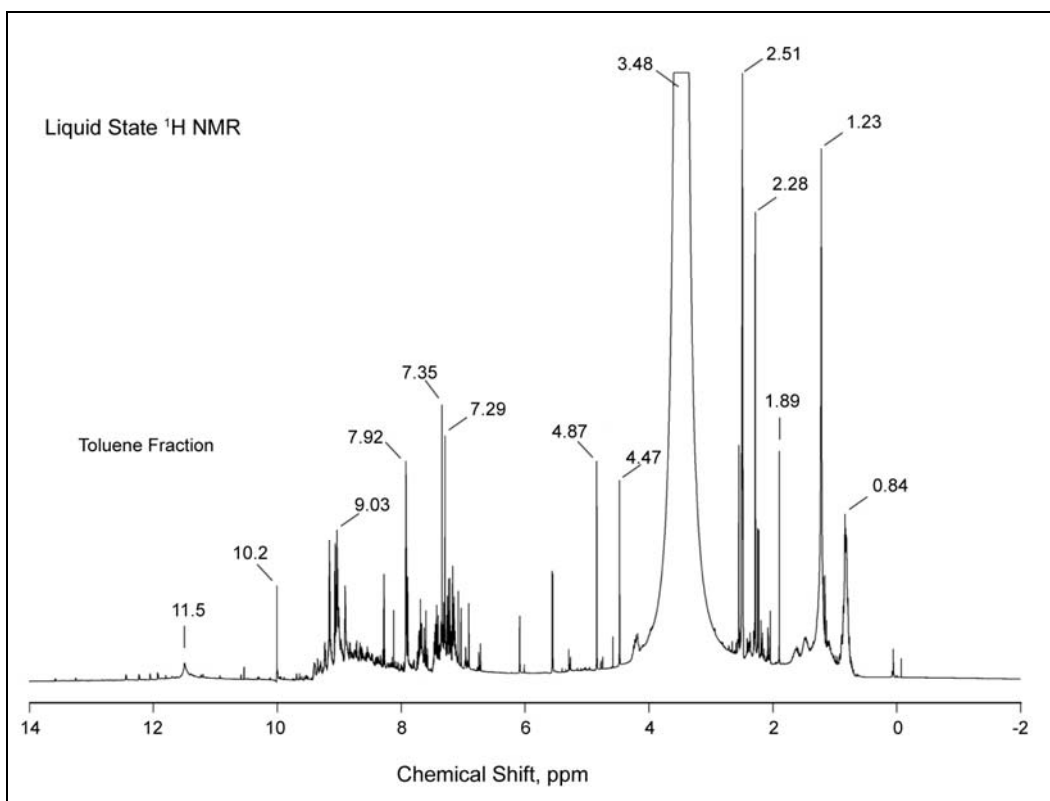


Figure 9. Liquid state  $^1\text{H}$  NMR spectrum of toluene fraction from  $\text{T}^{15}\text{NT}$  photolysate.

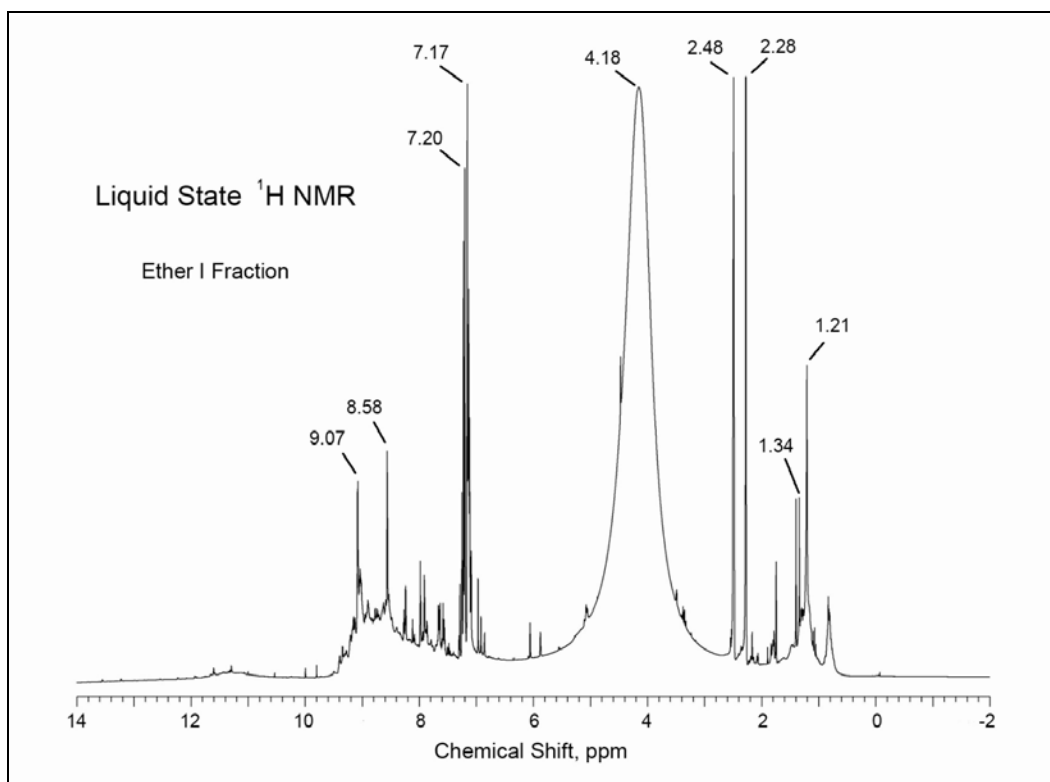


Figure 10. Liquid state  $^1\text{H}$  NMR spectrum of ether I fraction from  $\text{T}^{15}\text{NT}$  photolysate.

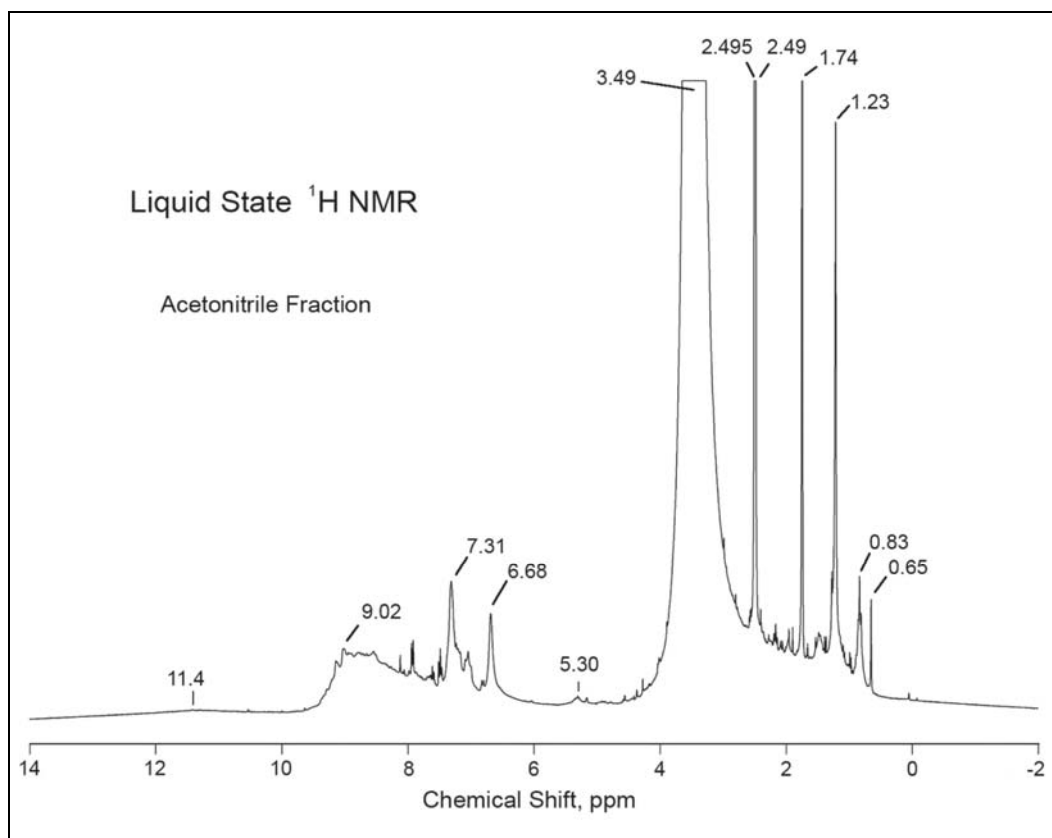


Figure 11. Liquid state  $^1\text{H}$  NMR spectrum of acetonitrile fraction from  $\text{T}^{15}\text{NT}$  photolysate.

spectra at approximately 10 ppm. Carboxylic acid protons were visible from 11 to 12 ppm in the individual plots of the  $^1\text{H}$  spectra (Figures 9-11). The  $^{15}\text{N}$  NMR spectra (Figure 12) of the ether I and acetonitrile fractions indicate that molecules containing similar functional groups are present in both fractions.

For example, azobenzene (510-508 ppm), residual nitro (364-361 ppm), azoxy (328-325 ppm), and amide (328-325 ppm) nitrogens are present in both fractions. The occurrence of azo and azoxy nitrogens in the acetonitrile fraction is consistent with the prediction of Burlinson et al. (1979a) that the insoluble residue is composed of oligomers of azo and azoxy compounds. The overall similarity of the spectra indicates that the solvent fractionation did not result in a significant separation of the photolysate components based upon class of functional group.

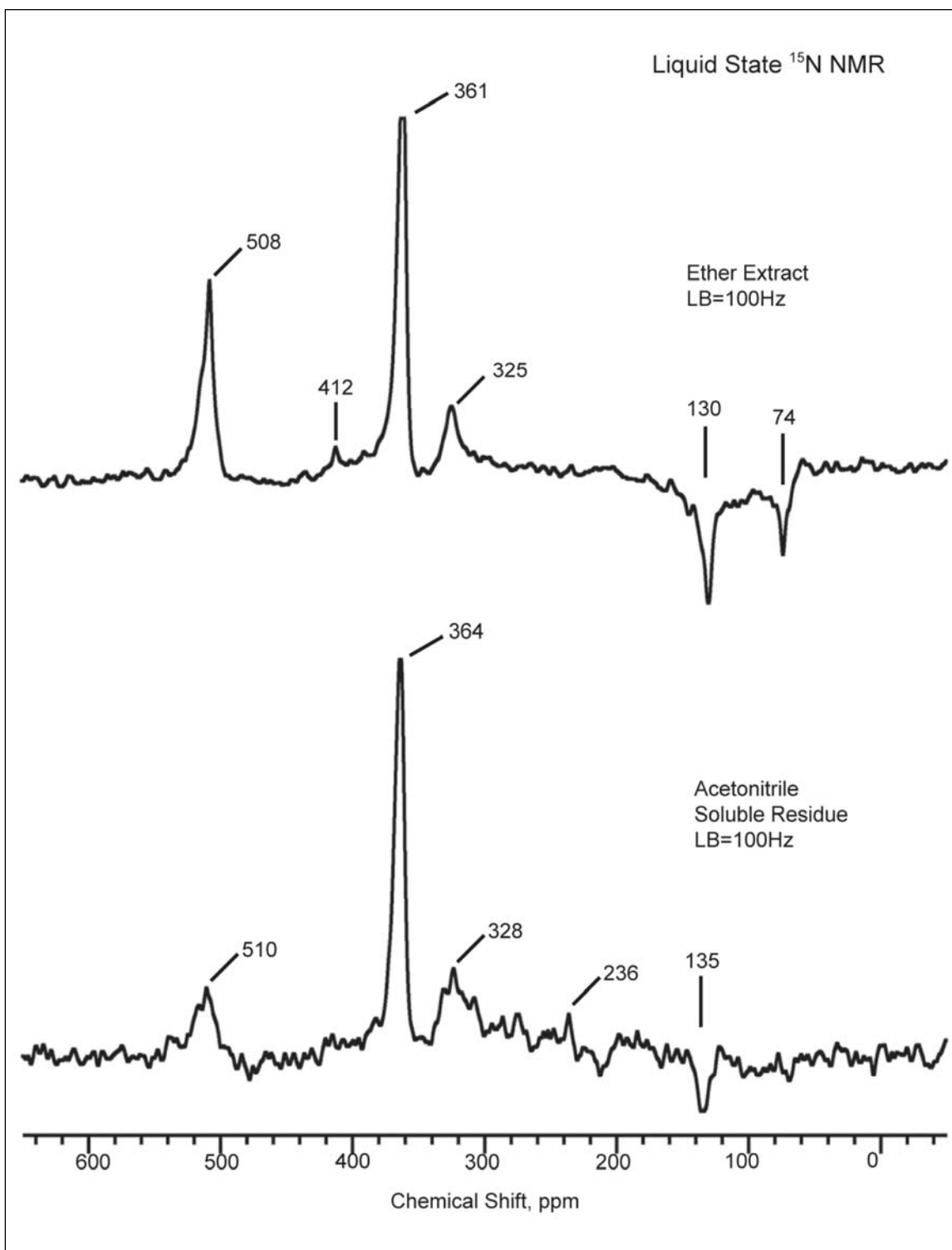


Figure 12. Liquid state acoustic  $^{15}\text{N}$  NMR spectra of solvent fractionated 1-hour  $\text{T}^{15}\text{NT}$  photolysate.

### Photodegradation of T<sup>15</sup>NT in presence of natural organic matter

Quantitative liquid state <sup>15</sup>N NMR spectra of 1-hour T<sup>15</sup>NT photolysates in the presence and absence of SRNOM are compared in Figure 13. The concentration of photodegradation products is less when T<sup>15</sup>NT is irradiated in the presence of the SRNOM. The azo (~ 510 ppm) and azoxy (~ 323 ppm) nitrogens are diminished in the spectrum of the T<sup>15</sup>NT/SRNOM photolysate. The distribution of nitrogens from 60 to 170 ppm also differs between the two spectra, with the amide nitrogens (133 ppm) diminished in the T<sup>15</sup>NT/SRNOM spectrum. It is important to note that the concentration of NOM in this experiment is high (approximately three times the high end of NOM in natural waters), and the results are not necessarily comparable to previous studies where *rates* of TNT photodegradation were measured in the presence of NOM. Further work will be necessary to determine whether absorption of light by the SRNOM decreased the rate of degradation product formation, or whether the presence of SRNOM caused an alteration in the photochemical degradation pathways of the TNT.

### Conclusions based on NMR analyses of aqueous-phase irradiations

The liquid state <sup>15</sup>N NMR spectrum of the 1-hour T<sup>15</sup>NT photolysate indicates that the most prominent nitrogen-containing functional groups in the degradation product mixture, after the unreacted nitro groups, are azoxy, amide, nitrile, and azo nitrogens. One of the challenges encountered by Burlinson et al. (1979a) in their original studies was the inability to chromatographically separate all components of the product mixture. Similar difficulties were encountered in our studies as the NMR spectrum suggests a mixture of such complexity that complete separation of all components is not possible without a major study devoted to this problem. Future NMR studies on TNT photolysis will need to compare results from UV lamp irradiation with direct sunlight, the effects of TNT concentration, and the photodegradation of TNT in natural waters.



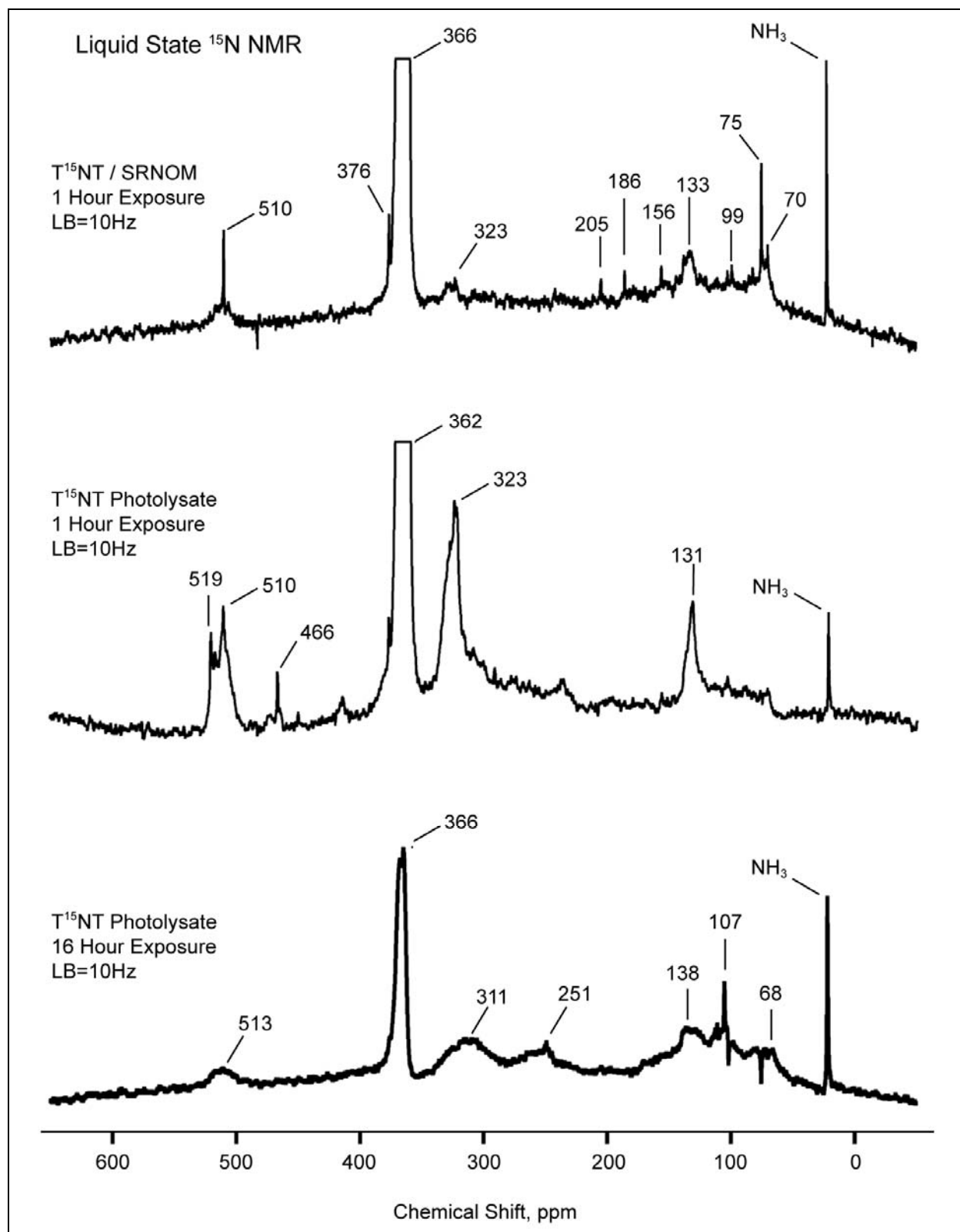


Figure 13. Liquid state inverse gated decoupled  $^{15}\text{N}$  NMR spectra of 1-hour  $\text{T}^{15}\text{NT}$  photolysates in presence and absence of SRNOM, and 16-hour  $\text{T}^{15}\text{NT}$  photolysate.

## Solid-phase irradiations

### Liquid chromatograph/mass spectrometry

#### *TNT treatments*

Ion chromatograms acquired for the *Dark Controls* and photolyzed TNT samples allow broad comparisons of the treatment conditions (Figure 14a-g). Peak heights and retention times for peaks in the chromatograms over three mass ranges of the *Dry TNT* treatment (Figure 14a) are similar to those observed for the *Wet TNT* treatment (Figure 14f). Peak heights and retention times for peaks in the chromatograms of the *Dry TNT Dark Control* (Figure 14b) and *Wet TNT Dark Control* (Figure 14g) exhibit more similarities to each other than to those acquired for the corresponding treated samples. Of the four experimental protocols for TNT, the *TNT Solution* treatment gave the simplest ion chromatograms with the fewest observed ion peaks, while *Dry TNT*, *TNT Solids*, and *Wet TNT* treatments generated more complex ion chromatograms with multiple ions observed below 600 mass units. The chromatograms of the *TNT Solution* treatment (Figure 14d) are consistent with those acquired for the *TNT Solution Dark Control* (Figure 14e), though the photolyzed sample chromatogram exhibits two small peaks before 10 min in the  $m/z$  300 to 400 mass range that are not observed in the *Dark Control*. The lower TNT peak abundances for the solution treatments at 15 days and the paucity of higher molecular weight species, as compared to the other treatments performed here, suggests more rapid decomposition in the solution form. Of the four experimental protocols for TNT, the *TNT Solution* treatment gave the simplest ion chromatograms, while *Dry TNT*, *TNT Solids*, and *Wet TNT* treatments generated more complex ion chromatograms with multiple ions observed below 600 mass units (Figure 14). The *TNT Solids* treatment (Figure 14c) exhibited the most complex ion chromatograms, and showed the presence of compounds not observed in the other preparations. Some ions were identified by mass-to-charge ratio ( $m/z$ ) and retention time as familiar TNT photolysis products such as aminodinitrobenzoic acid (ADNBA), isomers of dinitrotoluene (DNT) and aminodinitrotoluene (ADNT), TNB, and DNAn.

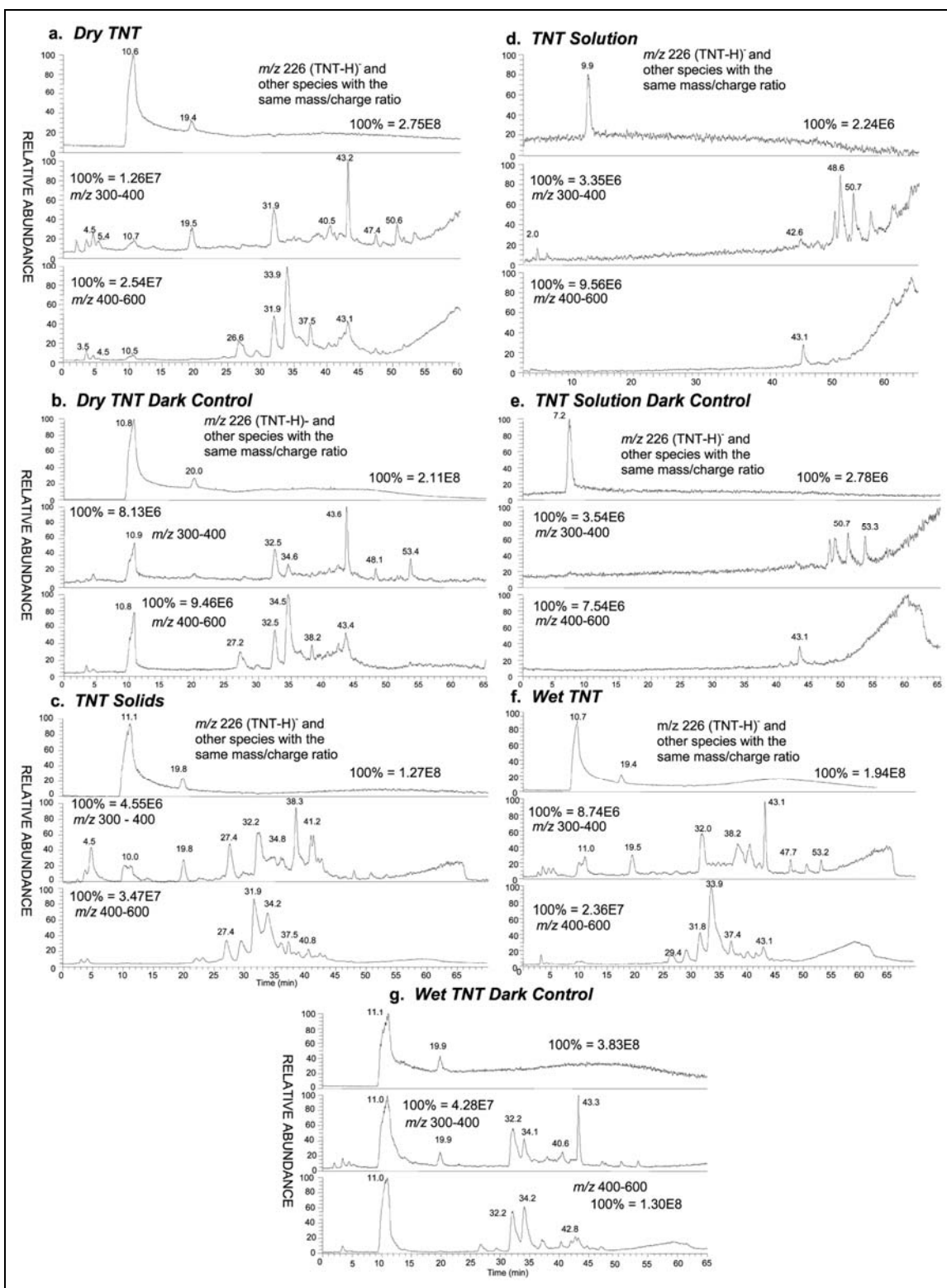


Figure 14. Ion profiles for selected anion of  $m/z$  226, anions in range of  $m/z$  300-400, and anions in range of  $m/z$  400-600 are presented for four representative TNT treatments. TNT loses a proton during electrospray ionization to yield an anion of  $m/z$  226. The traces show differences observed in samples with different initial preparation protocols at 15 days. Distance from light source was 122 cm.

Several ions observed in the 200-300 mass unit range and numerous other higher molecular weight ions eluting after TNT were not identified. For example, peaks for ions of  $m/z$  256 were observed at four separate retention times in some chromatograms, and only two of the retention times corresponded to ADNT isomers. The other peaks could correspond to the M-ion of the trinitrobenzaldoxime isomers, the (M-H)<sup>-</sup> ion of trinitrobenzoic acid, or ions related to other unknown products, but definitive identifications could not be made. Most identified ions were observed with abundances of 1 percent or less relative to the parent compound using area measurements from ion chromatograms and gave similar distributions over time as *Dark Controls*. Relative abundances for most ions were independent of distance from the light source and moisture levels.

The ion of  $m/z$  226, which, at the appropriate retention time, corresponds to the (M-H)<sup>-</sup> anion of ADNBA, was observed in the *Dry*, *Wet*, and *Solid TNT* treatments at abundances relative to TNT of approximately 3 percent and above. Relative abundances of ADNBA did not change substantially over distance or time, and were approximately equivalent to the values observed in the *Dark Controls* for samples other than the *TNT Solution* samples. The ion was not observed above approximately 0.001 percent relative abundance in the *TNT Solution* treatment, including the associated *Dark Controls*, at any time or distance. Therefore, if ADNBA formed in the *TNT Solution* treatment, the compound decomposed rapidly.

Differences between experimental protocols were also observed for the ion of  $m/z$  256, which corresponds to the acetate adduct (M + Ac - H)<sup>-</sup>, of the isomers 2ADNT and 4ADNT. The ion was observed at abundances relative to TNT of less than 1 percent in the *Dry*, *Wet*, and *Solid TNT* treatments. When observed in the *TNT Solution* samples, however, the ion abundances increased over time, with nearly 600 percent abundance relative to the concurrently decreasing abundance of TNT observed at 15 days for treatments that were 61 cm from the light. Treatments that were 61 cm from the light sources yielded the highest relative abundance for the ion of  $m/z$  256 at all time points after time zero, compared to treatments at either 10 cm or 122 cm from light sources (Figure 15). Abundance for the ion of  $m/z$  256 increased less in the *Dark Controls* than in the photolyzed treatments. The maximum abundance for the ADNT isomers relative to TNT in the *Dark Controls* was observed at 7 days. The data suggest that the ADNT isomers form through at least two pathways, and that the photolytic pathway occurs more rapidly than pathways occurring in the dark.

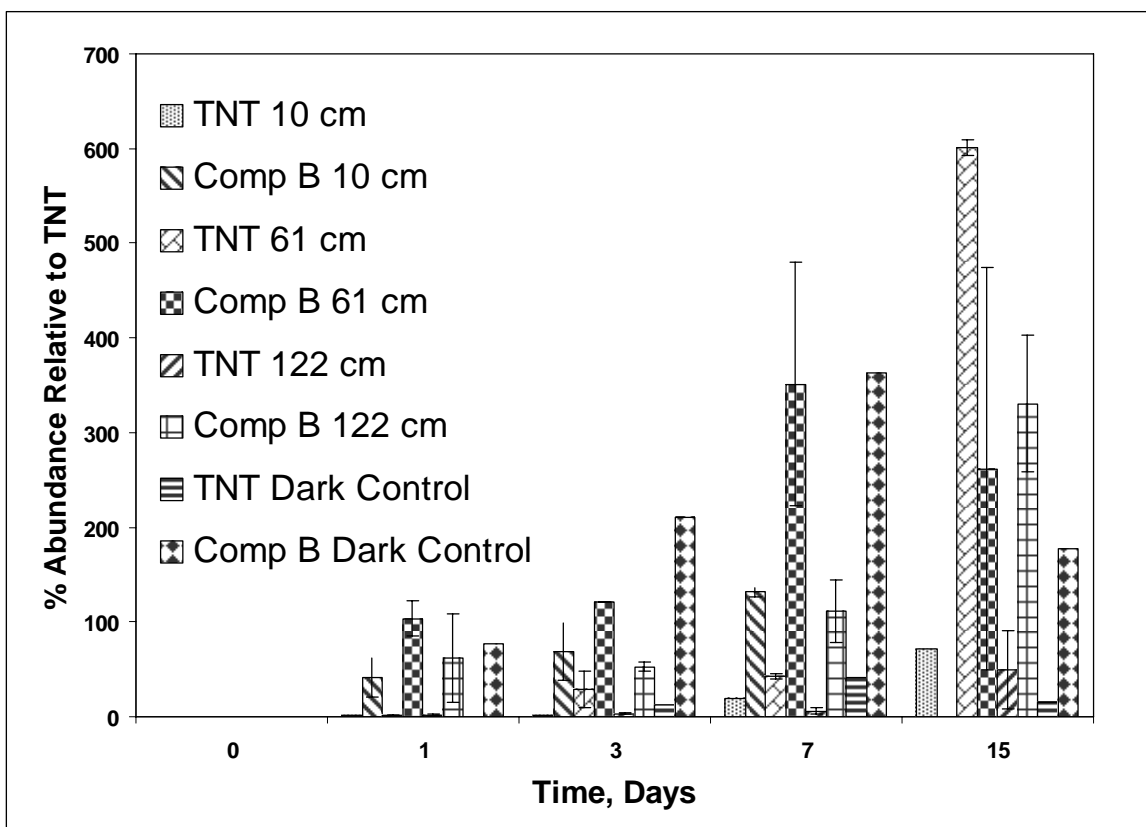


Figure 15. Abundance of ADNT isomers, the ion of  $m/z$  256, relative to TNT abundance, in *TNT Solution* and *Composition B (Comp B) Solution* controls and samples exposed to light for 15 days. The average relative abundance for the ion of  $m/z$  256 was <1 percent at time zero for both *TNT Solution* and *Composition B Solution* treatments.

Spectra acquired for *TNT solution* treatments demonstrate production of photolysis products over time. The spectrum generated from the TNT time zero control solution includes (TNT - H)<sup>-</sup> as the base peak, and ions of  $m/z$  196, (ADNT-H)<sup>-</sup>, and  $m/z$  256, (ADNT + Ac - H)<sup>-</sup>, at low relative abundances of approximately 2 percent each (Figure 16a). After 1 day, the deprotonated molecular anion (TNT - H)<sup>-</sup> continued as the base peak of a *TNT Solution* treatment 10 cm from light sources, and the relative abundances of the ADNT species increased to approximately 3 percent each (Figure 16b). The ions are observed in the corresponding *TNT Solution Dark Control* at less than 1 percent (Figure 16e). The spectrum acquired from a sample after 7 day exposure to light at 10 cm showed the relative increase in product ions associated with ADNT (Figure 16c); the abundance of the ion of  $m/z$  196 increased to 14 percent and the ion of  $m/z$  256 increased to 24 percent. An unidentified ion of  $m/z$  210 increased in abundance of approximately 2 percent at 1 day to 13 percent at 7 days.

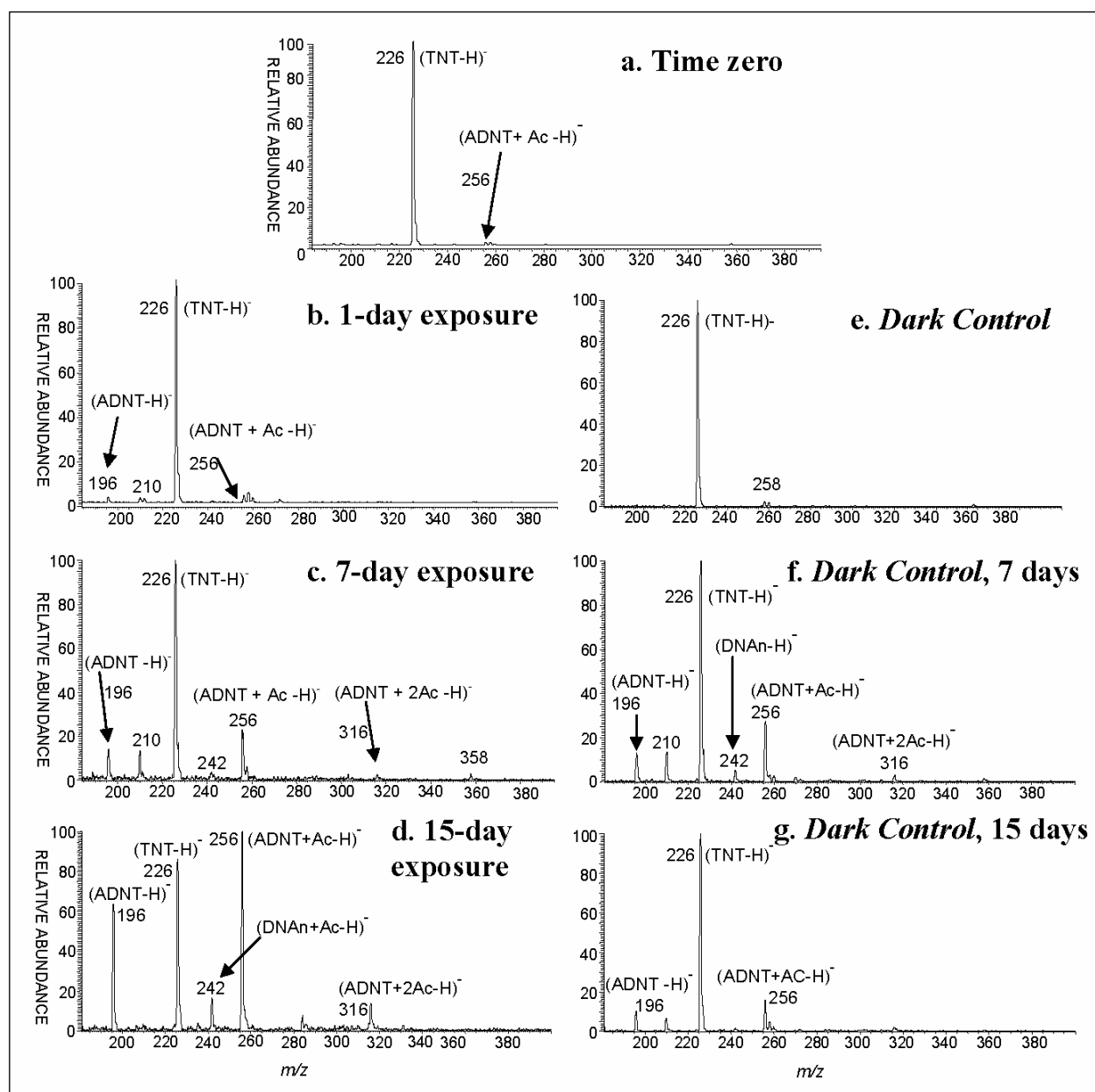


Figure 16. Selected spectra of *TNT Solution* treatments. Photolyzed samples were 10 cm from the light sources.

Other ions also were observed in the *TNT Solution* treatment after 7 days with abundances less than 2 percent: the ion of  $m/z$  242, which corresponds to the deprotonated acetate adduct of DNAn, and the ion of  $m/z$  316, which is an ADNT species formed by adduction of two molecules of acetic acid and loss of one proton,  $(ADNT + 2Ac - H)^-$ . The spectrum acquired for the *TNT Solution Dark Control* at 7 days gave the same ions with the DNAn peak and the ADNT-related species in greater abundance (Figure 16f). An unknown ion of  $m/z$  270 also appears in the *TNT Solution*

*Dark Control* and is not observed to the photolyzed sample. Amino dinitrotoluene was the predominant product after 15 days and was observed in three forms: adducts with one and two acetate species attached ( $m/z$  256 [100 percent] and  $m/z$  316 [14 percent], respectively), and the deprotonated molecular ion (77 percent) (Figure 16d). The deprotonated DNAn adduct with acetate, (DNAn + Ac - H)<sup>-</sup>, the ion of  $m/z$  242, was also observed in the *TNT Solution* treatment at 15 days exposure to light with 20 percent abundance relative to the base peak. The *TNT Solution Dark Control* at 15 days was little changed from the 7-day *Dark Control* (Figure 16g).

#### *RDX treatments*

The ion current profiles produced upon analysis of the RDX preparations were much simpler and showed far fewer peaks than those observed for the TNT preparations. Mass spectrometric analysis of the soils and solids from photolysis experiments and controls with RDX showed that HMX and hexahydro-1-nitroso-3,5-dinitro-1,3,5-triazine (MNX) were both present. HMX was observed as the (M + Ac - H)<sup>-</sup> species of  $m/z$  355. MNX was observed as the (M + Ac - H)<sup>-</sup> species of  $m/z$  265. The *Wet RDX* treatments including *Dark Controls* yielded HMX with an average abundance of  $7.9 \pm 2.0$  percent, and MNX with an abundance of  $1.1 \pm 0.3$  percent, relative to the abundance of RDX. For the *RDX Solids* treatments, HMX was observed in abundances varying from 0.13 to 1.2 percent, while MNX was observed in abundances ranging from 0.045 to 1.7 percent. Exposure to light did not affect the abundance of HMX or MNX.

An unknown ion of  $m/z$  264 was observed in both sets of RDX treatments at abundances of less than 1 percent relative to RDX. The unknown ion of  $m/z$  264 corresponds in mass to the acetate adduct of a molecular species potentially with the chemical formula C<sub>3</sub>H<sub>5</sub>N<sub>6</sub>O<sub>5</sub>. The relative abundance of this ion showed an increase in the *RDX Solids* treatments at 61 cm and 122 cm from the light sources for 7 days (Figure 17). The abundance returned to less than 0.4 percent relative to RDX abundance in the solid samples by Day 15. Photolytic influence on the abundance of the ion in the solid samples was not significant. The ion showed little change related to time, distance, or light in the *Wet RDX* treatment. The *RDX Solids Dark Controls* yielded similar results.

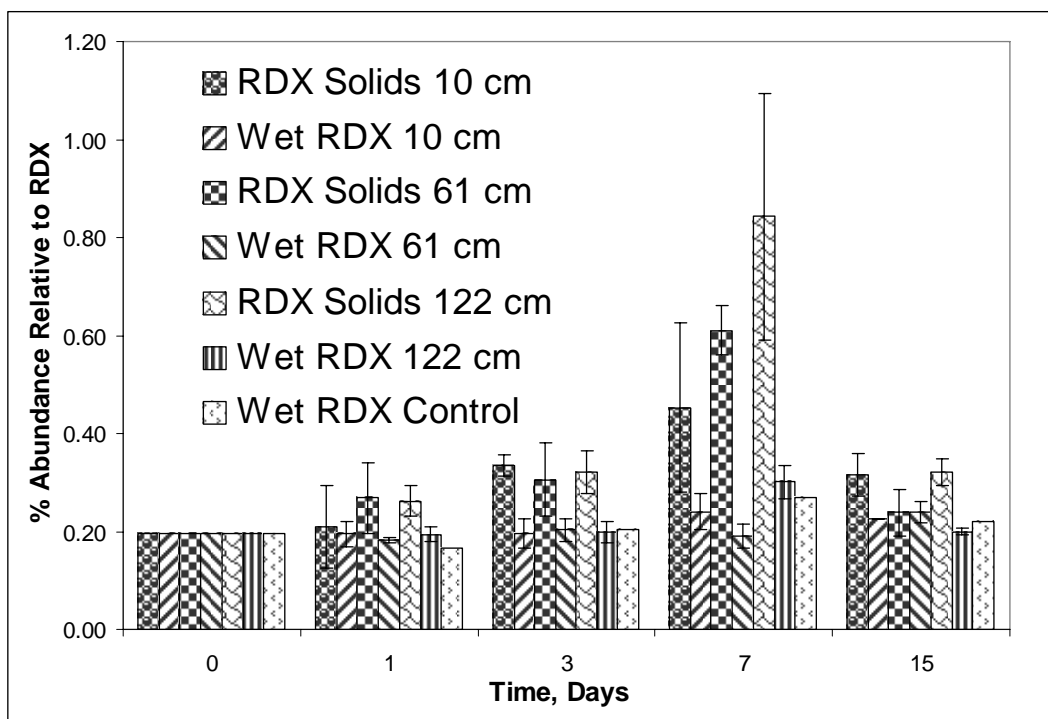


Figure 17. Abundance of unknown ion of  $m/z$  264 relative to RDX in photolysis of *RDX Solids* and *Wet RDX*.

The RDX ring cleavage product methylene dinitramine was observed in low relative abundance ( $\sim 0.003$  percent) in the *Wet RDX* treatments and *Dark Controls*. A second ring cleavage product of RDX, 4-nitro-2,4-diazabutanol, was not detected. An unknown ion of  $m/z$  484 was present in the *RDX Solids* treatments at all times and distances. The ion was observed at approximately 1 percent relative abundance in the 1 day treatments at all distances, increased to approximately 8 percent at 7 days, and maintained that abundance in treatments exposed to the light source for 15 days.

#### Composition B treatments

Photolysis of Composition B residues was investigated for solids mixed with a wet slurry, as a solid, and as a solution applied to dry soil to form a wet slurry. Both TNT and RDX were detected in most Composition B treatments, though TNT was not observed in some *Composition B Solution* treatments collected on Day 15. Military grade Composition B is 59.5 percent RDX, 39.5 percent TNT, and 1 percent wax. If no reaction occurred, the relative abundance of TNT in Composition B treatments would be approximately 66.4 percent of the abundance observed for RDX. Treatments did not exhibit as much TNT relative to RDX as predicted,



however. The *Wet Composition B* treatments gave an average value of  $41.4 \pm 9.6$  percent for TNT abundance relative to RDX abundance, while the solids samples yielded an average abundance of  $27.7 \pm 8.6$  percent for TNT relative to RDX abundance. The *Composition B Solution* treatments showed the greatest deviation from the predicted ratio with an abundance of TNT to RDX of only  $2.4 \pm 0.9$  percent for samples collected prior to Day 15. The Day 15 *Composition B Solution* treatment gave highly variable results with no detectable TNT in two of the samples from plates 61 cm from the light,  $3.9 \pm 0.12$  percent TNT in the 15-day treatments at 10 cm, and TNT abundances from 0.75–10,000 percent of RDX abundances in the remaining four treatments. The *Composition B Solution* treatments that yielded extraordinarily high TNT abundances may have been contaminated from glass plates used previously with TNT slurries. If the potentially contaminated samples are excluded as anomalies, the data demonstrate that TNT decomposes upon photolysis at a faster rate than does RDX, and that TNT decomposition occurs more readily in the finely divided, high surface area conditions created in the *TNT Solution* and *Composition B Solution* treatments. Decomposition in the *Solid* treatments without soil occurred less rapidly than in the *Solution* treatments. The slowest decomposition of TNT in Composition B was observed for the *Wet Composition B* treatment. The comparatively rapid decomposition of TNT in the *Composition B Solution* treatment versus the other treatment conditions is consistent with the results observed for TNT decomposition in the *TNT Solution* treatment.

#### *Comparisons of TNT, RDX, and Composition B treatments*

Other ions observed in TNT or RDX treatments were also observed in the treatments with Composition B. 2ADNT and 4ADNT were observed in both *Composition B Solution* and *TNT Solution* treatments (Figure 15). The combined relative abundance of the ADNT isomers was greater in *Composition B Solution* treatments than in *TNT Solution* treatments at all distances and times, with one exception; at Day 15, the relative abundance of ADNT in the *TNT Solution* treatments 61 cm from the light source exceeded the relative abundance in the corresponding *Composition B* treatment at the same distance. The data suggest that photolytic decomposition of TNT in the *Composition B Solution* treatments occurred more rapidly than in the *TNT Solution* treatments, whereas generation of products from TNT in *Composition B Solids* treatments occurs only slightly more readily than in *TNT Solids*.

The ion of  $m/z$  226, which corresponds to the deprotonated ADNBA anion, followed similar trends in the Composition B treatments as in the analogous TNT treatments. Aminodinitrobenzoic acid was not detected in the *Composition B Solution* or the *TNT Solution* treatments. The ion was observed with a relative abundance range of approximately 2 to 4 percent in the *Composition B Solids* treatments, while its relative abundance in the *TNT Solids* treatments was approximately 4 to 8 percent (Figure 18).

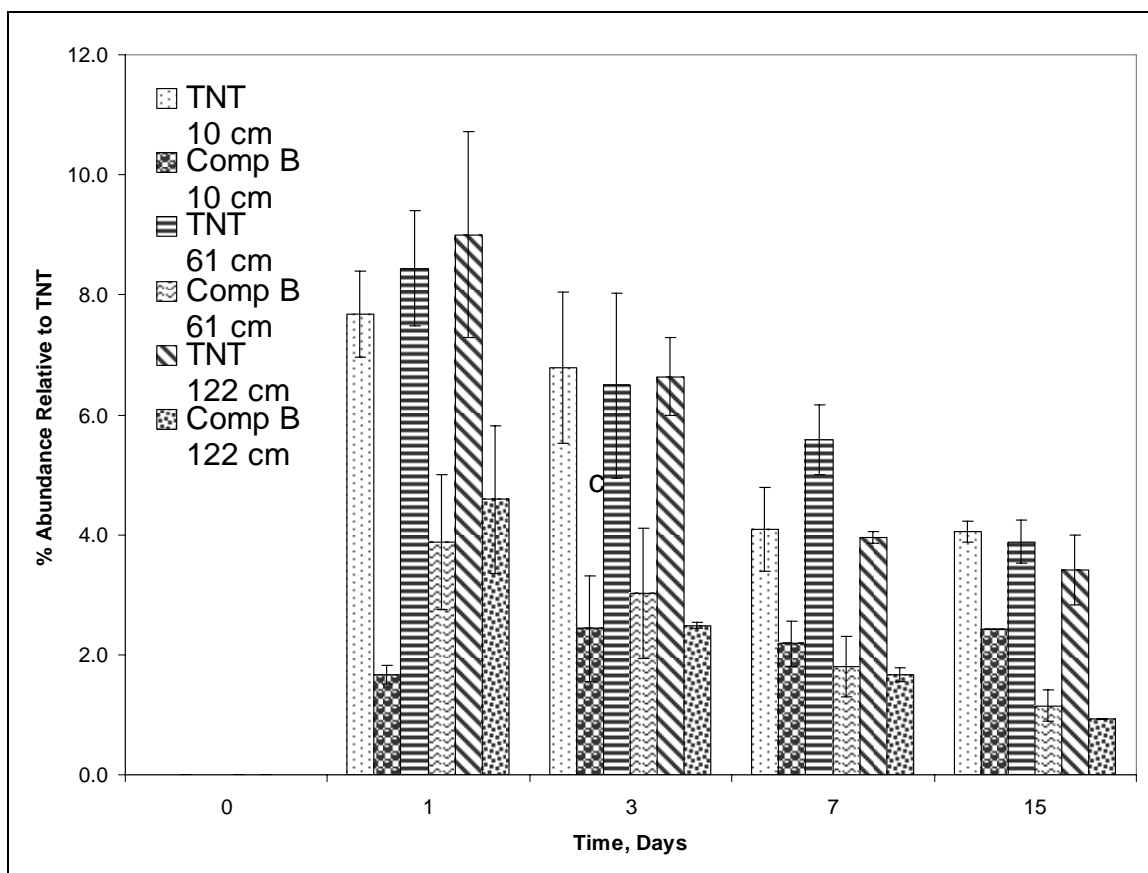


Figure 18. Abundance of aminodinitrobenzoic acid as the anion  $m/z$  226, relative to TNT in *TNT Solids* and *Composition B (Comp B) Solids* treatments exposed to light for 15 days. The ion was not detected at time zero.

Spectra for the *Composition B Solution* treatments demonstrated more rapid TNT decomposition compared to the rate in *TNT Solution* treatments. As with the *TNT Solution* sample (Figure 16A), the (TNT-H)<sup>-</sup> ion dominated the spectrum of the time zero sample of Composition B (Figure 19a). The ion of  $m/z$  256, the acetate adduct of ADNT, was not observed with the *Composition B Solution* at time zero, though it was observed with the *TNT Solution* at that time. At Day 1, two ADNT anionic species,  $m/z$  196 and  $m/z$  256, were observed in *Composition B Solution*

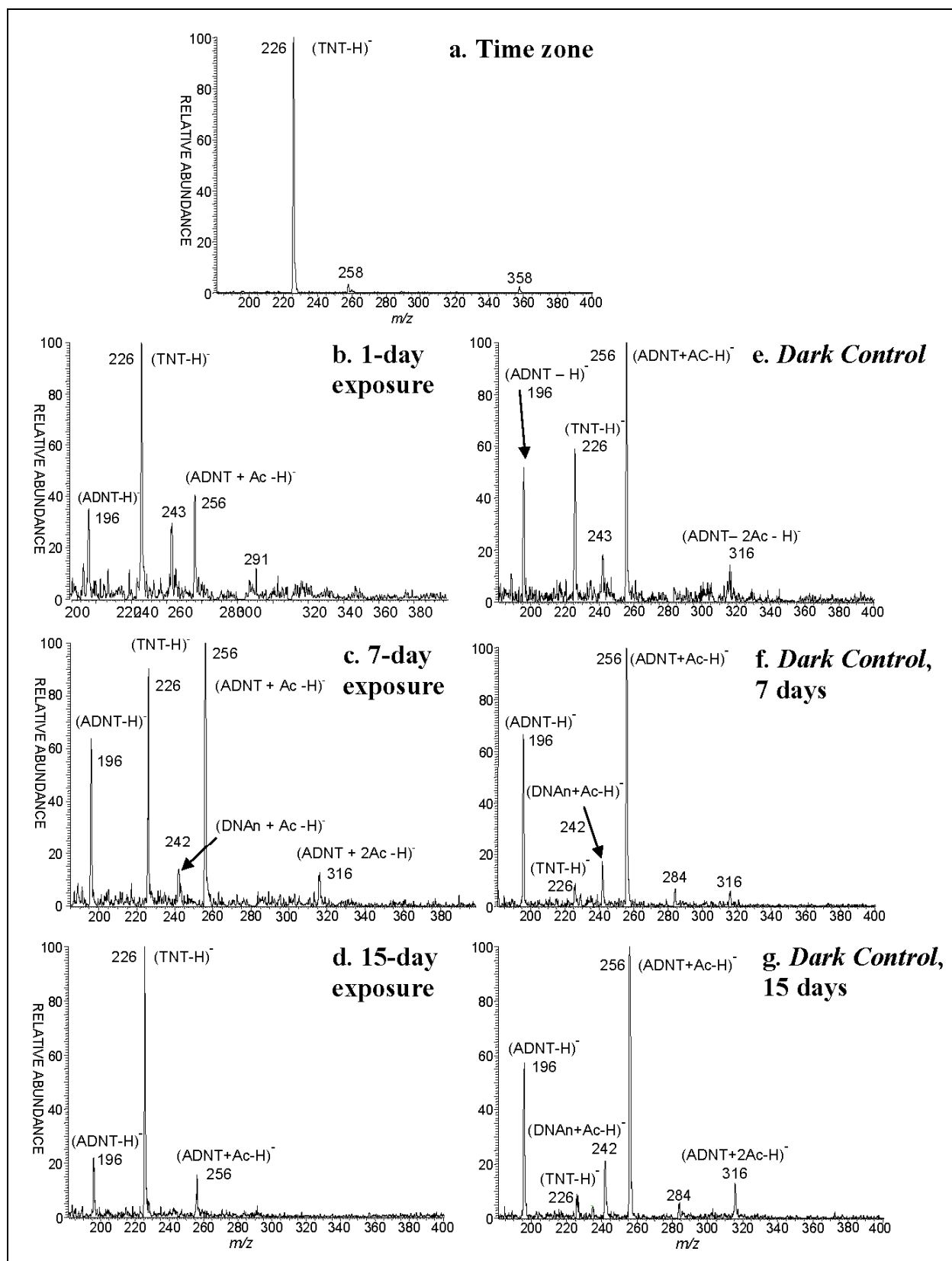


Figure 19. Selected spectra of *Composition B Solution* treatments. Photolyzed samples were 10 cm from light sources.

treatments 10 cm from the light sources, at approximately 35- and 42-percent abundance, respectively, relative to the ion of  $m/z$  226 (TNT-H)<sup>-</sup> (Figure 19b). The ions appeared in greater abundance in the *Composition B Dark Control* at Day 1 (Figure 19E); however, the ion of  $m/z$  256 was the base peak. The same two ADNT species were observed in the spectrum for the *TNT Solution* treatment, but in significantly lower abundance (Figure 16b). An unknown ion of  $m/z$  243 was observed in both the photolyzed *Composition B Solution* sample and *Dark Control* at Day 1. This ion was not observed in the *TNT Solution* sample or *Dark Control* (Figure 16e).

At Day 7, three ADNT species were observed in the *Composition B Solution* spectrum (Figure 19a), suggesting increased abundance of ADNT at that time compared to the abundance at Day 1 when only two ADNT species were observed. The DNAn acetate adduct,  $m/z$  242, was also observed after 7 days of photolytic exposure at approximately 17 percent abundance relative to the base peak, the ion of  $m/z$  256. The ion was also observed in the *Composition B Solution Dark Control* (Figure 19f) and also in the *TNT Solution* (Figure 16c) treatment and *Dark Control* (Figure 16f), but at lower abundances than in the *Composition B Solution* spectra. The deprotonated TNT molecular anion was observed at 91 percent abundance for the *Composition B Solution* treatment at Day 7, but at only 8 percent relative abundance in the corresponding *Dark Control*. Interestingly, the TNT species is the base peak in the *TNT Solution* treatment and *Dark Control* at Day 7 rather than the ion of  $m/z$  256 as is observed for *Composition B*. An unknown ion of  $m/z$  284 was observed in the *Composition B Solution Dark Control* at Day 7, and also at Day 15, but not in the corresponding photolyzed samples. The ion of  $m/z$  284 was not observed until Day 15 for the photolyzed *TNT Solution* sample. The ion was not detected in the *TNT Solution Dark Control*.

At Day 15, the ADNT species abundances decreased with respect to the TNT species for the photolyzed *Composition B Solution* treatment (Figure 19d). The spectrum from the *Dark Control* for the *Composition B Solution* treatment exhibited little difference from that acquired for the Day 7 *Dark Control*. At Day 15 for the *TNT Solution* treatment, the relative abundances of the observed species were approximately equal to the abundances observed for the *Composition B Solution* treatment at Day 7. As with the *Composition B Solution Dark Control*, the *TNT Solution Dark Control* gave similar results at Day 7 and Day 15. The abundance of the

(TNT-H)<sup>-</sup> ion was 100 percent in the *TNT Solution Dark Control* (Figure 16g), but only 10 percent for the *Composition B Solution Dark Control* (Figure 19g).

#### *Conclusions based on LC/MS analyses*

Generation of photolysis products of Composition B and military grade TNT and RDX with soil depends on the physical form of the explosive and moisture. Photolysis of TNT, whether alone or as a component of Composition B, generated products more readily than RDX under all conditions. TNT and Composition B in solution applied to soils exhibited faster decomposition and product formation than was observed for solid explosive alone or mixed with soil.

The data also indicate that TNT undergoes more rapid decomposition as a component of Composition B from solution than when it is deposited onto soil from a TNT-only solution. TNT was depleted from some *Composition B Solution* samples at Day 15, but was detected in all 15-day *TNT Solution* samples. Also, ion abundances in spectra from *TNT Solution* samples at Day 15 were similar to the abundances of the same ions at only Day 7 from the *Composition B Solution* samples.

When mixed with soil, TNT underwent photolytic decomposition more rapidly in dry conditions than in wet conditions. In addition to known photolysis products such as ADNT and ADNBA, *TNT Solids* and *Composition B Solids* yielded numerous unidentified products. Since explosive residues from low-order detonations are likely to occur in solid form in the environment, these reactions may constitute an important fate process on training ranges.

This study demonstrates that photolytic decay of TNT and Composition B occurs most readily under low moisture, high surface area conditions. Thus factors such as wind that may disperse solid explosive materials as small particles may also facilitate photodegradation.

## **Nuclear magnetic resonance spectrometry**

### **TNT, RDX, and Composition B solids treatments**

The solid state <sup>13</sup>C NMR spectrum of *TNT Solids* treatment showed parent TNT only; no signals were visible in the solid state <sup>15</sup>N spectrum,

presumably because the sample was not labeled with  $^{15}\text{N}$ . The spectrum for *RDX Solids* exhibited the parent RDX peak at 61.5 ppm and a peak at 29.7 ppm (Figure 20). The later peak does not appear to correspond to photochemical degradation products as it was present in the solid state spectrum of the starting material. The identity of the peak is uncertain. It is not visible in the liquid state  $^{13}\text{C}$  NMR spectrum of the starting RDX. The solid state  $^{15}\text{N}$  NMR chemical shift of TNT is 366 ppm. The liquid state chemical shifts of RDX are 349.0 ppm for the nitro group and 182.4 ppm for the ring nitrogen, respectively. The solid state  $^{15}\text{N}$  NMR chemical shifts of the ring nitrogens in RDX are at 197.5 and 175.4 ppm (data not shown). The solid state  $^{15}\text{N}$  NMR spectrum of the light exposed Composition B exhibits a major peak at 125.2 ppm (Figure 21). The very strong signal-to-noise ratio is surprising given that the sample is not labeled with  $^{15}\text{N}$ . A comparable mass of unlabeled TNT by itself subjected to a 15-day exposure showed no signals in the solid state  $^{15}\text{N}$  NMR. Additionally, nitrogen signals in the solid state NMR of the unlabelled RDX standard were not detected. The chemical shift position of 125.2 ppm occurs in the amide region. Signals were detected at 124.5 to 127.5 ppm in the liquid state  $^{15}\text{N}$  NMR spectrum of degradation products from aqueous phase photolysis of  $^{15}\text{N}$  ring labeled RDX subjected to irradiation in a solar simulator. After solid state NMR analysis, the combined sample of replicates 4, 5, and 6 (*Composition B Solids* treatment) were dissolved in deuterated ( $^3\text{H}$ ) DMSO and analyzed by liquid state  $^{13}\text{C}$  NMR analysis (Figure 22). The spectrum shows only the parent Composition B components. The peaks at 61.2 and 63.3 ppm correspond to RDX and HMX, respectively. The peaks at 14.9 ppm (methyl carbon), 122.5 ppm (C3 and C5), 132.9 ppm (C1), 145.6 ppm (C4), and 150.8 ppm (C2 and C6) correspond to TNT. In conclusion, although the solid state  $^{15}\text{N}$  NMR spectrum of the exposed Composition B suggests the possibility of degradation products, the liquid state  $^{13}\text{C}$  spectrum shows no indication of degradation products.

### **TNT solution treatment**

No discreet resonances due to TNT could be observed in the spectrum of the whole soil prior to extraction. The  $^{13}\text{C}$  NMR revealed the presence of acetic acid, but no TNT or identifiable TNT degradation products in the acetonitrile extract.

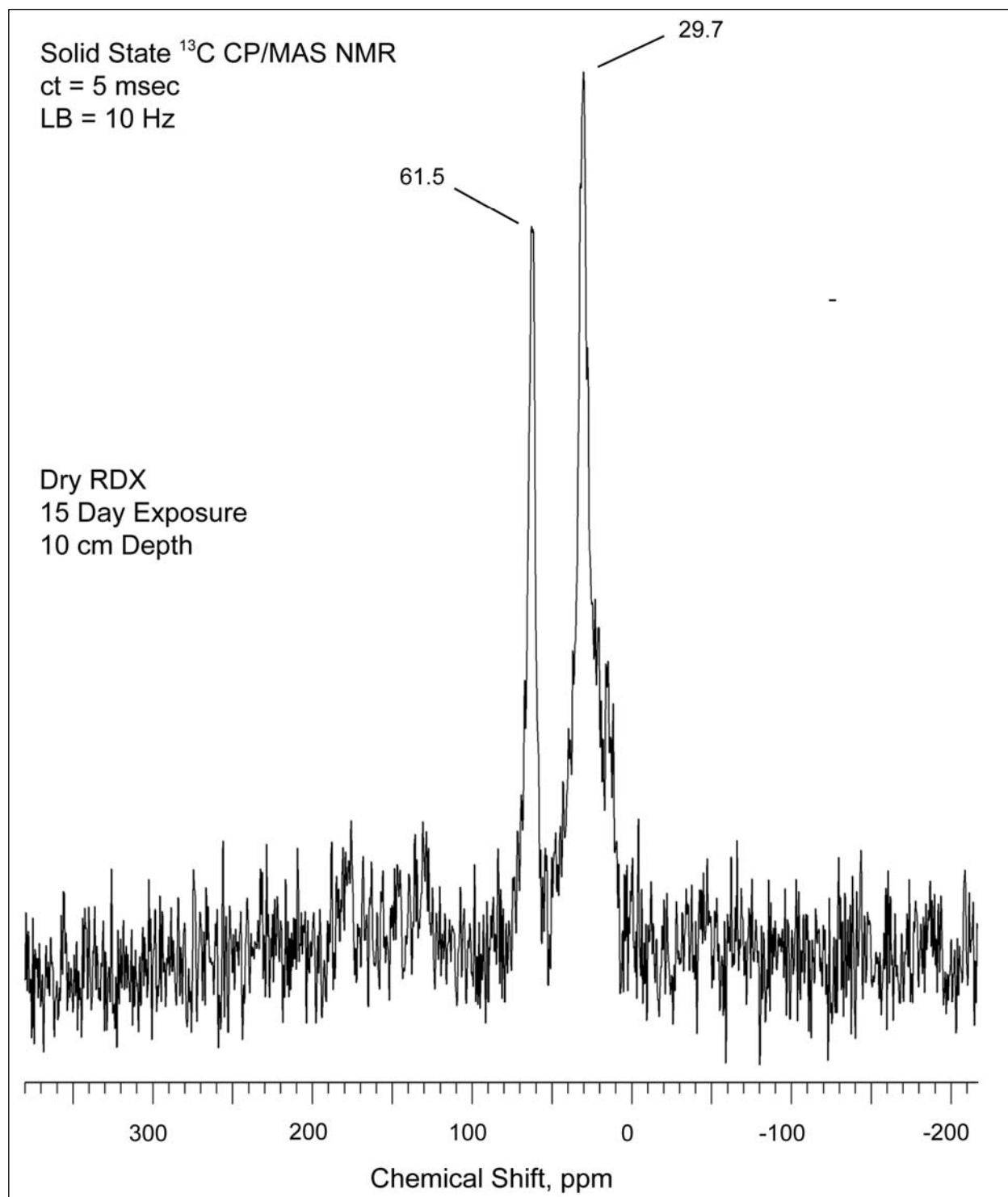


Figure 20. Solid state CP/MAS  $^{13}\text{C}$  NMR of dry, solid RDX exposed to light for 15 days at 10-cm depth.

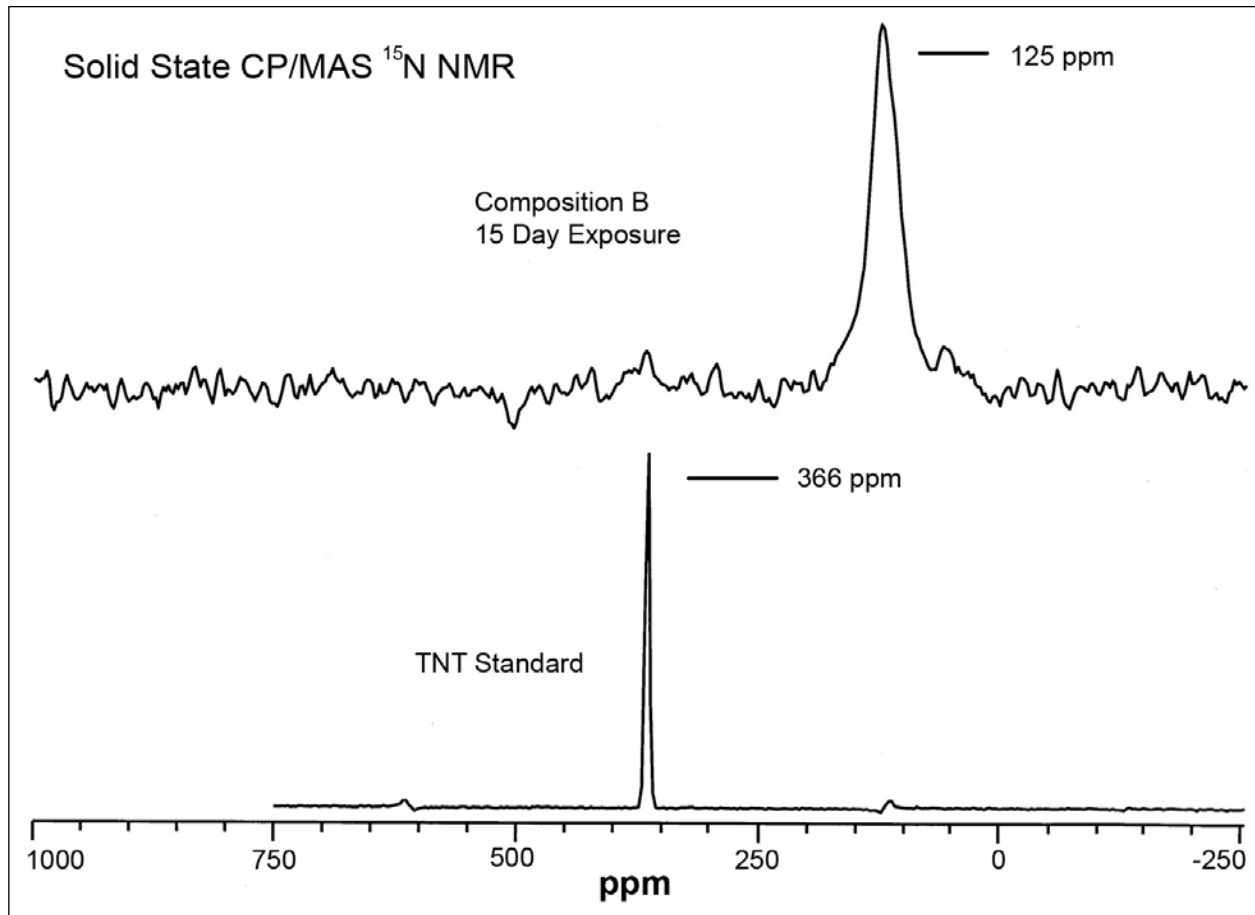


Figure 21. Solid state CP/MAS  $^{15}\text{N}$  NMR spectra of  $^{15}\text{N}$ -labeled TNT standard and unlabeled Composition B subjected to 15-day light exposure.



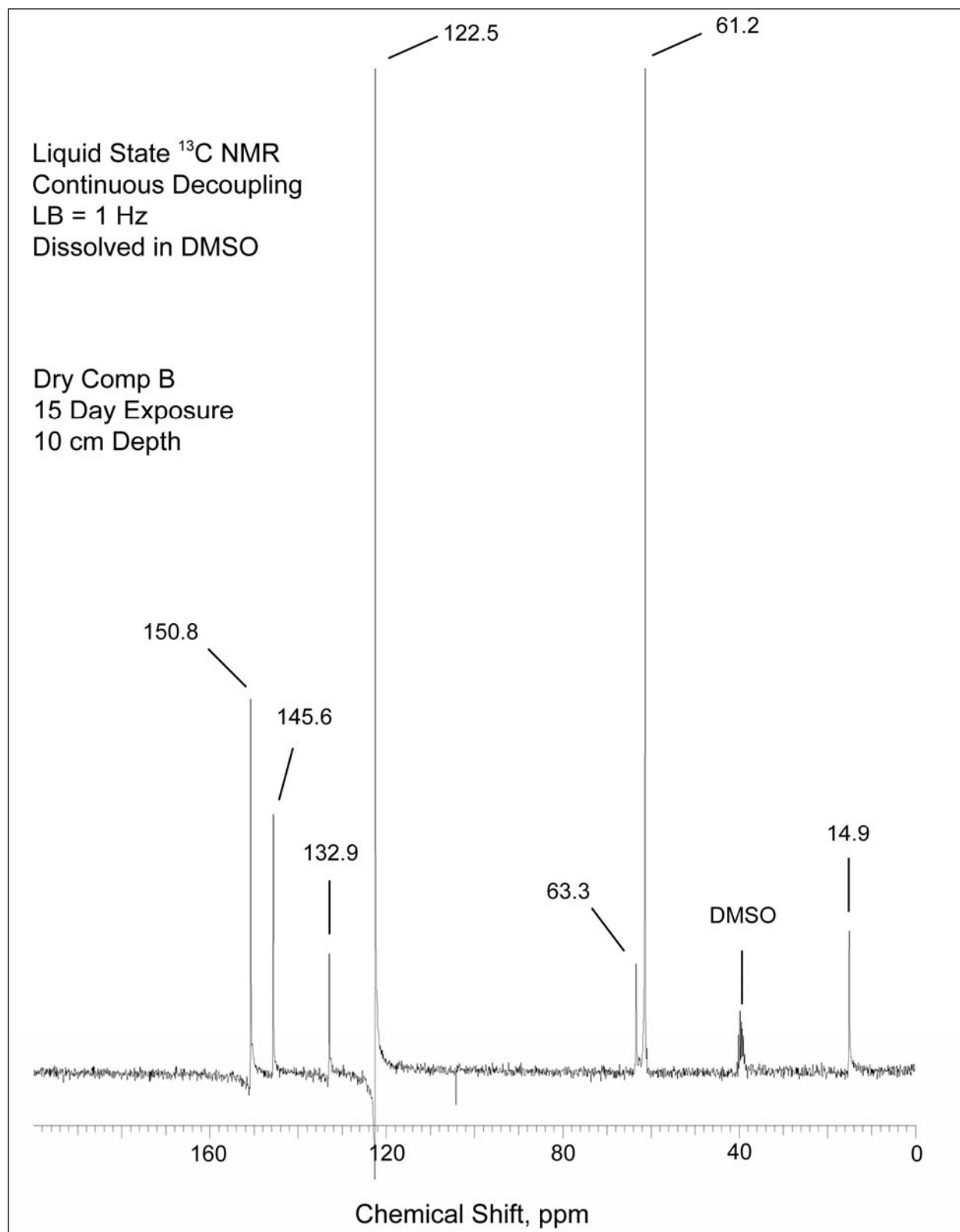


Figure 22. Liquid state  $^{13}\text{C}$  NMR of dry, solid Composition B exposed to light for 15 days at 10-cm depth.

## 4 Conclusions

The rate of photolysis over a 16-hr period of irradiation was relatively rapid. Analyses of  $^{13}\text{C}$  CP/MS NMR spectra at 1-, 4-, 8-, and 16-hour irradiation of TNT in solution indicated increases in the proportion of carboxylic acid groups and aliphatic alcohol carbons. Furthermore, methyl carbons were converted to methylene, alcohol, and carboxylic acid carbons over the same time period, while the aromatic  $\text{C}_4$  carbon was resistant to chemical alteration. Nitro groups continued to be lost from 1 through 16 hours. Results of LC/MS analyses indicated that the acetate adduct of mono amino dinitrotoluenes also increased over time (15 days) as TNT decreased. The rate of TNT photolysis was much faster than the rate for RDX. Although relatively few RDX photoproducts were observed using LC/MS, at least two unidentified products peaked at Day 7. Although HMX and a transformation product of RDX (MNX) were present in RDX, exposure to light had no observable effect on their relative abundance by LC/MS analysis. Relative abundances of most ions observed in all treatments were independent of light intensity or moisture. Many of the ions identifiable by LC/MS from TNT treatments were also present in dark controls; however, the photolytic pathway was faster.

Irridation of TNT in the aqueous phase generated dramatically more photolysis products than have been previously reported. Results of liquid state  $^{15}\text{N}$  NMR indicated that the most prominent nitrogen-containing functional groups, exclusive of unreacted nitro groups, were azoxy, amide, nitrile, and azo nitrogens. The spectra corresponded to many of the previously identified photolysis products of TNT. Judging from the broad peaks observed, the number of constituents in the insoluble residue was an order of magnitude or greater than the 16 constituents identified. Results of liquid state  $^{13}\text{C}$  spectral analyses on TNT, RDX, and Composition B solids treatments showed no degradation products, probably due to low relative abundance resulting in insufficient sensitivity of this methodology. Except for an unidentified peak in the RDX solids treatment, no photolysis products were observed in solids treatments of TNT, RDX, or Composition B or in the treatment for which TNT solution was introduced to soils.

Results of LC/MS analyses yielded numerous unidentified and identifiable products. TNT, alone and as a component of Composition B, generated

products more readily than RDX under all conditions. Photolysis was faster when TNT was mixed with soil. These results are consistent with previously reported results in water where dissolved organic carbon promoted photolysis of TNT. Treatments in which TNT and Composition B were introduced to soils in solution exhibited faster photolysis than occurred with solid alone or in treatments in which TNT was introduced to soils as a solid. Production of photoproducts from TNT as a component of Composition B in solution occurred more rapidly than with TNT-only solution. These results suggest that Composition B photolysis, particularly the TNT component, generates a dynamic mixture of products and ions, even from the solid.

## References

- Bedford, C. D., P. S. Carpenter, and M. P. Nadler. 1996. *Solid-State Photodecomposition of Energetic Nitramines (RDX and HMX)*. NAWCWPNS TP 8271. China Lake, CA: Naval Air Warfare Center Weapons Division.
- Brannon, J. M., and J. C. Pennington. 2002. *Environmental fate and transport process descriptors for explosives*. ERDC/EL TR-02-10. Vicksburg, MS: U.S. Army Engineer Research and Development Center.
- Burlinson, N. E. 1980. *Fate of TNT in an aquatic environment: Photodecomposition vs. biotransformation*. TR 79-445. Silver Spring, MD: Naval Surface Weapons Center.
- Burlinson, N. E., L. A. Kaplan, and C. E. Adams. 1973. *Photochemistry of TNT: Investigation of the "pink water" problem*. NOLTR 73-172. Silver Spring, MD: Naval Ordnance Laboratory, White Oak.
- Burlinson, N. E., M. E. Sitzmann, D. J. Glover, and L. A. Kaplan. 1979a. *Photochemistry of TNT and related nitroaromatics: Part III*. NSWC/WOL TR 78-198. Silver Spring, MD: Naval Surface Weapons Center.
- Burlinson, N. E., M. E. Sitzmann, L. A. Kaplan, and E. Kayser. 1979b. Photochemical generation of the 2,4,6-trinitrobenzyl anion. *Journal of Organic Chemistry* 44(21): 3695-3698.
- Glover, D. J., and J. C. Hoffsomer. 1979. *Photolysis of RDX in aqueous solution, with and without ozone*. Technical Report 78-175, ADA080195, Silver Spring, MD: Naval Surface Weapons Center.
- Godejohann, M., M. Astratov, A. Preiss, K. Levsen, and C. Muegge. 1998. Application of continuous-flow HPLC-proton-nuclear magnetic resonance spectroscopy for the structural elucidation of phototransformation products of 2,4,6-trinitrotoluene. *Analytical Chemistry* 70: 4104-4110.
- Hawari, J., A. Halasz, C. Groom, S. Deschamps, L. Paquet, C. Beaulieu, and A. Corriveau. 2002. Photodegradation of RDX in aqueous solution: A mechanistic probe for biodegradation with *rhodococcus* sp. *Environmental Science and Technology* 36: 5117-5123.
- Just, C. L. and J. L. Schnoor. 2004. Phytphotolysis of hexahydro-1,3,5-triazine (RDX) in leaves of reed canary grass. *Environmental Science and Technology* 38(1): 290-295.
- Kaplan, L. A., N. E. Burlinson, and M. E. Sitzmann. 1975. *Photochemistry of TNT: investigation of the "pink water" problem, Part II*. NSWC-1155. Silver Spring, MD: Naval Surface Weapons Center.
- Kubose, D. A., and J. C. Hoffsomer. 1977. *Photolysis of RDX in aqueous solution: Initial studies*. Technical Report 77-20, ADA042199. Silver Spring, MD: Naval Surface Weapons Center.

- Lewis, T. A., D. A. Newcombe, and R. L. Crawford. 2004. Bioremediation of soils contaminated with explosives. *Journal of Environmental Management* 70: 291-307.
- Mabey, W. R., D. Tse, A. Baraze, and T. Mill. 1983. Photolysis of nitroaromatics in aquatic systems. I. 2,4,6-trinitrotoluene. *Chemosphere* 12(1): 3-16.
- Pennington, J. C., K. Poe, B. Silverblatt, C. A. Hayes, and S. A. Yost. 2006. Explosive residues from low-order detonations of artillery munitions, Chapter 9, In *Distribution and fate of energetics on DoD test and training ranges: Interim Report 6*. ERDC TR-06-12. Vicksburg, MS: U.S. Army Engineer Research and Development Center.
- Pennington, J. C., T. F. Jenkins, G. Ampleman, S. Thiboutot, J. M. Brannon, J. Clausen, A. D. Hewitt, S. Brochu, P. Dubé, J. Lewis, T. A. Ranney, D. Faucher, A. Gagnon, J. A. Stark, P. Brousseau, C. B. Price, D. J. Lambert, A. Marois, M. Bouchard, M. E. Walsh, S. L. Yost, N. M. Perron, R. Martel, S. Jean, S. Taylor, C. Hayes, J. M. Ballard, M. R. Walsh, J. E. Mirecki, S. Downe, N. H. Collins, B. Porter, and R. Karn. 2004. *Distribution and fate of energetics on DoD test and training ranges: Interim Report 4*. ERDC TR-04-4. Vicksburg, MS: U.S. Army Engineer Research and Development Center.
- Pennington, J. C., T. F. Jenkins, G. Ampleman, S. Thiboutot, J. M. Brannon, J. Lewis, J. E. Delaney, J. Clausen, A. D. Hewitt, M. A. Hollander, C. A. Hayes, J. A. Stark, A. Marois, S. Brochu, H. Q. Dinh, D. Lambert, R. Martel, P. Brousseau, N. M. Perron, R. Lefebvre, W. Davis, T. A. Ranney, C. Gauthier, S. Taylor, and J. M. Ballard. 2003. *Distribution and fate of energetics on DoD test and training ranges: Interim Report 3*. ERDC TR-03-2. Vicksburg MS: U.S. Army Engineer Research and Development Center.
- Pennington, J. C., T. F. Jenkins, G. Ampleman, S. Thiboutot, J. M. Brannon, J. Lynch, T. A. Ranney, J. A. Stark, M. E. Walsh, J. Lewis, C. A. Hayes, J. E. Mirecki, A. D. Hewitt, N. Perron, D. Lambert, J. Clausen, and J. J. Delfino. 2002. *Distribution and fate of energetics on DoD test and training ranges: Interim Report 2*. ERDC TR-02-8. Vicksburg, MS: U.S. Army Engineer Research and Development Center.
- Pennington, J. C., T. F. Jenkins, G. Ampleman, S. Thiboutot, J. Clausen, A. D. Hewitt, J. Lewis, M. R. Walsh, M. E. Walsh, T. A. Ranney, B. Silverblatt, A. Marois, A. Gagnon, P. Brousseau, J. E. Zufelt, K. Poe, M. Bouchard, R. Martel, D. D. Walker, C. A. Ramsey, C. A. Hayes, S. L. Yost, K. L. Bjella, L. Trepanier, T. E. Berry, D. J. Lambert, P. Dubé, and N. M. Perron. 2005. *Distribution and fate of energetics on DoD test and training ranges: Interim Report 5*. ERDC TR-05-2. Vicksburg, MS: U.S. Army Engineer Research and Development Center.
- Pennington, J. C., T. F. Jenkins, J. M. Brannon, J. Lynch, T. A. Ranney, T. E. Berry, Jr., C. A. Hayes, P. H. Miyares, M. E. Walsh, A. D. Hewitt, N. Perron, and J. J. Delfino. 2001. *Distribution and fate of energetics on DoD Test and training ranges: Interim Report 1*. ERDC TR-01-13. Vicksburg, MS: U.S. Army Engineer Research and Development Center.
- Peyton, G. R., M. H. LeFaivre, and S. W. Maloney. 1999. *Verification of RDX photolysis mechanism*. CERL Technical Report TR 99/93, ADA371755. Champaign, IL: U.S. Army Engineer Research and Development Center.

- Rosenblatt, D. H., E. P. Burrows, W. R. Mitchell, and D. L. Parmer. 1991. Organic explosives and related compounds, *The Handbook of Environmental Chemistry*. O. Hutzinger, Springer-Verlag. 3 Part G, 195-234.
- Spanggord, R. J., W. R. Mabey, T.-W. Chou, and J. H. Smith. 1985. Environmental fate of selected nitroaromatic compounds in the aquatic environment. *Chem. Ind. Inst. Toxicol. Ser.* 15-32.
- Spanggord, R. J., T. Mill, T. W. Chou, R. W. Mabey, W. H. Smith, and S. Lee. 1980. Environmental fate studies on certain munition wastewater constituents, Final Report, Phase I – Literature review. ADA082372. Stanford Research Institute, Menlo Park, CA for U.S. Army Medical Research and Development Command, Fort Detrick, Frederick, MD.
- Talmage, S. S., D. M. Opresko, C. J. Maxwell, C. J. E. Welsh, F. M. Cretella, F. M., P. H. Reno, and F. B. Daniel. 1999. Nitroaromatic munition compounds: Environmental effects and screening values. *Reviews of Environmental Contamination and Toxicology* 161: 1-156.

# REPORT DOCUMENTATION PAGE

*Form Approved*  
*OMB No. 0704-0188*

Public reporting burden for this collection of information is estimated to average 1 hour per response, including the time for reviewing instructions, searching existing data sources, gathering and maintaining the data needed, and completing and reviewing this collection of information. Send comments regarding this burden estimate or any other aspect of this collection of information, including suggestions for reducing this burden to Department of Defense, Washington Headquarters Services, Directorate for Information Operations and Reports (0704-0188), 1215 Jefferson Davis Highway, Suite 1204, Arlington, VA 22202-4302. Respondents should be aware that notwithstanding any other provision of law, no person shall be subject to any penalty for failing to comply with a collection of information if it does not display a currently valid OMB control number. **PLEASE DO NOT RETURN YOUR FORM TO THE ABOVE ADDRESS.**

<b>1. REPORT DATE (DD-MM-YYYY)</b> September 2007		<b>2. REPORT TYPE</b> Final report		<b>3. DATES COVERED (From - To)</b>	
<b>4. TITLE AND SUBTITLE</b>  Photochemical Degradation of Composition B and Its Components				<b>5a. CONTRACT NUMBER</b>	
				<b>5b. GRANT NUMBER</b>	
				<b>5c. PROGRAM ELEMENT NUMBER</b>	
<b>6. AUTHOR(S)</b>  Judith C. Pennington, Kevin A. Thorn, Larry G. Cox, Denise K. MacMillan, Sally Yost, and Randy D. Laubscher				<b>5d. PROJECT NUMBER</b>	
				<b>5e. TASK NUMBER</b>	
				<b>5f. WORK UNIT NUMBER</b>	
<b>7. PERFORMING ORGANIZATION NAME(S) AND ADDRESS(ES)</b>  See reverse.				<b>8. PERFORMING ORGANIZATION REPORT NUMBER</b>  ERDC/EL TR-07-16	
<b>9. SPONSORING / MONITORING AGENCY NAME(S) AND ADDRESS(ES)</b> Strategic Environmental Research and Development Program Arlington, VA 22203				<b>10. SPONSOR/MONITOR'S ACRONYM(S)</b>	
				<b>11. SPONSOR/MONITOR'S REPORT NUMBER(S)</b>	
<b>12. DISTRIBUTION / AVAILABILITY STATEMENT</b>  Approved for public release; distribution is unlimited.					
<b>13. SUPPLEMENTARY NOTES</b>					
<b>14. ABSTRACT</b> Products of photodecomposition of 2,4,6-trinitrotoluene (TNT) have been observed as a coating on TNT particles and as a fine powdered residue surrounding TNT particles on ranges receiving limited rainfall. The significance of photolysis of explosive formulations on training ranges is unknown. Therefore, photolysis of a common explosive formulation, Composition B, and its components in a soil matrix were evaluated. Objectives included determination of photolysis rates, effects of light intensity and duration, effects of moisture on photolysis, and identification of photolysis products. Irradiations were performed in laboratory microcosms under controlled conditions. Solutions, solids, and both solutions and solid explosives spiked into soils were irradiated. Two approaches were used to characterize products: liquid chromatography/mass spectrometry and a combination of solid and liquid state <sup>13</sup> C and <sup>15</sup> N nuclear magnetic resonance (NMR), and liquid state <sup>1</sup> H NMR. Irradiation of TNT in the aqueous phase generated dramatically more photolysis products than were previously reported. The most prominent nitrogen-containing functional groups, exclusive of unreacted nitro groups, were azoxy, amide, nitrile, and azo nitrogens. Results suggest that Composition B photolysis, particularly the TNT component, generates a dynamic mixture of products and ions beginning on the solid surfaces before dissolution, and increasing once in solution phase.					
<b>15. SUBJECT TERMS</b> Composition B Explosives		HMX LC/MS NMR	Photochemistry Photodegradation Photolysis	RDX TNT	
<b>16. SECURITY CLASSIFICATION OF:</b>			<b>17. LIMITATION OF ABSTRACT</b>	<b>18. NUMBER OF PAGES</b>  63	<b>19a. NAME OF RESPONSIBLE PERSON</b>
<b>a. REPORT</b> UNCLASSIFIED	<b>b. ABSTRACT</b> UNCLASSIFIED	<b>c. THIS PAGE</b> UNCLASSIFIED			<b>19b. TELEPHONE NUMBER (include area code)</b>

**7. (Concluded)**

U.S. Army Engineer Research and Development Center  
Environmental Laboratory  
3909 Halls Ferry Road, Vicksburg, MS 39180-6199;

National Water Quality Laboratory  
U.S. Geological Survey  
PO Box 25046  
Denver Federal Center, Bldg 95, MS 408  
Denver, CO 80225;

Spec Pro  
4815 Bradford Drive, Suite 201, Huntsville, AL 35805